Electronic Supplementary Material (ESI) for Materials Advances.

Supporting Information

Enhancing photoluminescence of conjugated nanoparticles through graft polymer architectures

Ashley E. Masucci[1], Masoud Ghasemi[1], Christian W. Pester[1,2,3], and Enrique D. Gomez[1,2,4]

[1]Department of Chemical Engineering, The Pennsylvania State University, University Park, PA 16802
[2]Department of Materials Science and Engineering, The Pennsylvania State University, University Park, PA 16802
[3]Department of Chemistry, The Pennsylvania State University, University Park, PA 16802
[4]Materials Research Institute, The Pennsylvania State University, University Park, PA 16802

Corresponding Authors
*edg12@psu.edu
*pester@psu.edu

1 Table of Contents

2 General material information

3-bromothiophene, hexanes, n-butyllithium in hexanes, 1,6-dibromohexane, tetrahydrofuran (THF), diethyl ether, magnesium sulfate ($MgSO_4$), n-bromosuccinimide (NBS), N,N-dimethylformamide (DMF), sodium chloride (NaCl), 2,5-Dibromo-3-hexylthiophene, isopropyl magnesium chloride (i-PrMgCl), hydrochloric acid, methanol, acetone, [1,3-bis(diphenylphosphino)propane]dichloronickel(II) (Ni(dppp)Cl2) (CAS: 15629-92-2), chloroform, sodium azide, dichloromethane (DCM), trimethylsilyl-2-propyn-1-ol, trimethylamine, 2-bromoisobutyryl bromide, heptane, ethyl acetate, methyl methacrylate (MMA), tris(2-phenylpyridinato-C2,N)iridium(III) ($Ir(ppy)_3$), Poly(ethylene glycol) methyl ether, propargyl bromide, trimethylsilylacetylene (CAS: 1066-54-2), bis(triphenylphosphine)palladium(II) dichloride ($Pd(PPh_3)_2Cl_2$) copper iodine (CuI), tetrabutylammonium fluoride solution 1.0 M in THF (TBAF), copper bromide (CuBr), N,N,N',N'',N'' Pentamethyldiethylenetriamine (PMDETA) were purchased from Sigma-Aldrich and used as received (unless otherwise noted). Standard grade silica gel was purchased from Sorbent Technologies and used as received.

3 General analytical information

Nuclear magnetic resonance (NMR) spectra were recorded using a Bruker AVIII-HD-500 MHz instrument. All 1H NMR experiments are reported in δ units, parts per million (ppm), and were normalized to the signal for the deuterated solvent $CDCl_3$ (7.26 ppm).

Gel permeation chromatography (GPC) spectrum were recorded using TOSOH EcoSEC Elite High performance GPC system equipped with a refractive index detector and an absorption detector. The TOSOH system was run with THF as the eluant at 1.0 mL/min and a TSKgel H Type column as the solid phase. Linear polystyrene standards were used as calibration for molecular weight. GPC was also performed on an Agilent 1260 system with an Agilent PLgel-MIXED-LC column running chlorobenzene as the eluant. The Agilent system was equipped with a refractive index detector (RID), viscometer (VS), light scattering detector (LS), and multiwavelength detector (MWD). Chlorobenzene was run at 0.5 mL/min and the detectors were calibrated with linear polystyrene standards (Agilent EasiVial PS-M).

Matrix-assisted laser desportion/ionization-time of flight (MADLI-TOF) mass spectrometry (MS) was performed using a Bruker ultrafleXtreme MALDI-TOF/TOF in high-resolution, reflectron positive mode to determine isotope splitting. The sample was prepared at a concentration of 0.5 mg/mL and mixed with a dithranol matrix. The sample was spotted on a MTP 384 ground steel target plate and loaded into the machine. The measurement was taken under high vacuum.

Fourier transform infrared (FTIR) spectroscopy was performed in attenuated total reflection (ATR) mode on a Bruker Tensor 27 FTIR. The solid polymer sample was placed on a germanium crystal.

UV-vis spectroscopy was measured on an Agilent Technologies Cary 60 UV-Vis spectrophotometer with 1 cm quartz cuvettes. Solid-state absorbance samples were prepared by spin coating a 1 mg/mL solution onto a quartz slide.

Steady-state fluorescent emission spectra were measured at an excitation wavelength of 450 nm on a Photon Technology International QuantaMaster 300 fluorimeter equipped with a Xe arc lamp and a 914 photomultiplier detection system. The liquid samples were loaded into a 1 cm quartz cuvette and emission was recorded at 90° from excitation. The quantum yields were measured by calculating the linear slope of integrated fluorescence to absorbance and comparison to a standard of known quantum yield, 4-(dicyanomethylene)-2-methyl-6-(4-dimethylaminostyryl)-4H-pyran ($\phi = 0.35$ in chloroform) [1].

Differential scanning calorimetry (DSC) was performed on a Texas Instruments Q2000 DSC. Using alumina pans, the polymer and reference were loaded in the DSC. The temperature was ramped from RT-200 ^{o}C at a rate of 20 ^{o}C/min, then cooled at 10 ^{o}C/min to -50 ^{o}C, then reheated to 200+ ^{o}C at a rate of 10 ^{o}C/min. The second heating curve was used to calculate thermal transitions (T_g, T_m).

Nanoparticle size characterization DLS was performed on a Malvern Zetasizer Nano ZS equipped with a 4 mW diode laser (λ = 632.8 nm). The size was obtained by measuring the Brownian motion of the particles, fitting the autocorrelation function and using the Stokes-Einstein equation. PDI, a measure of the average uniformity of the nanoparticles, was obtained as the square of the standard deviation divided by the z-averaged diameter of the nanoparticles. Because (PT-g-PMMA)NP shows some evidence of aggregation after multiple days, the size of (PT-g-PMMA)NP was measured on a separate batch as the rest of the studies presented here, to allow for the use of a fresh solution and ensure minimal aggregation.

4 Synthetic procedure for conjugated backbones

4.1 Synthesis of poly(3-hexylthiophene-co-3-(bromohexyl thiophene))

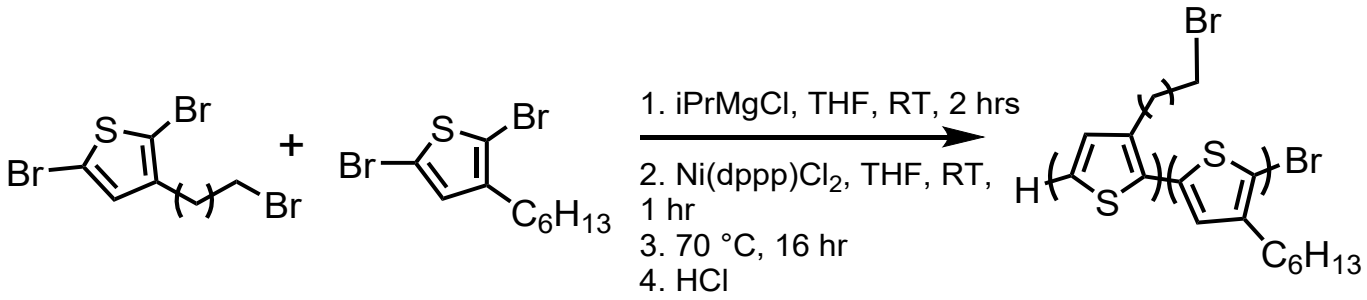

(161 mg, 0.49 mmol) 2,5-Dibromo-3-hexylthiophene and (200 mg, 0.49 mmol) 2,5-dibromo-3-(6-bromohexyl)-thiophene were loaded into a 20 mL dry vial with a stir bar. The solution was purged and added to a glovebox under Ar. Dry THF (2 mL) was added, followed by dropwise addition of i-PrMgCl (2 M, 1.11 mmol, 0.55 mL)) and stirred for 1 h at room temperature. The solution was added all at once to a separate 20 mL vial containing Ni(dppp)Cl2 and dry THF (7.2 mL) and stirred at room temperature for 1 hour, then heated to 70 °C overnight. The reaction mixture was quenched with 5% HCl, precipitated in methanol. Soxhlet was performed with methanol, acetone, hexanes, and chloroform. The chloroform fraction was concentrated under reduced pressure and dried under vacuum. (Yield: 85%) ^{1}H NMR (500 MHz, $CDCl_3$) d 7.00 (s, 1H), 3.44 (t, $BrCH_2$, 2H (58%)), 2.83 (t, CH_2, 2H), 1.92-1.25 (m, CH_2, 8H), 0.94 (1, CH_3, 3H (42%)).

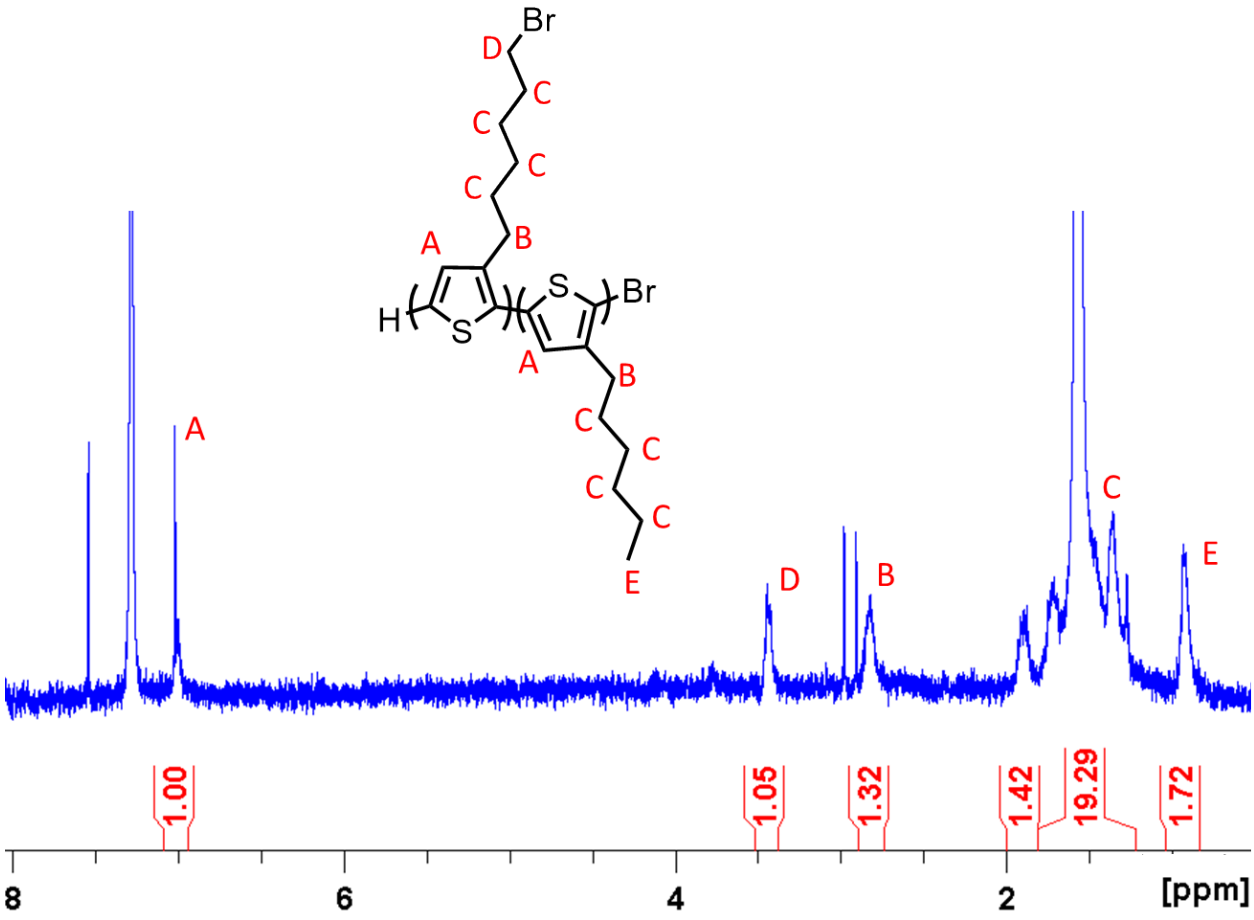

Figure S1: ^{1}H NMR spectra ($CDCl_3$) for poly(3-hexylthiophene-co-3-(bromohexyl thiophene)).

4.2 Synthesis of poly(3-hexylthiophene-*co*-3-(azidohexyl thiophene))

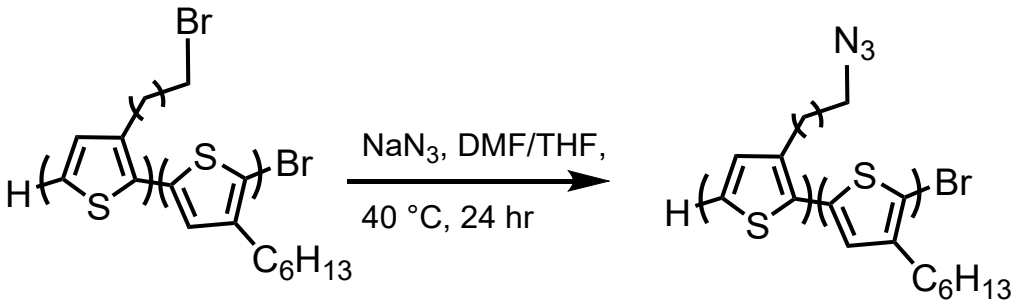

100 mg (0.268 mmol bromine groups, 1 equiv.) poly(3-hexylthiophene-*co*-3-(bromohexyl thiophene)) was added to a oven dried 20 mL vial with a stir bar. 1.74 g (2.68 mmol, 10 equiv.) sodium azide was added to the vial and dissolved in 1 mL DMF and 1 mL THF. The reaction was stirred at room temperature overnight. The reaction was precipitated in MeOH, filtered, rinsed with water, and dried under vacuum to obtain poly(3-hexylthiophene-*co*-3-(azidohexyl thiophene)). (84% yield) ^{1}H NMR (500 MHz, $CDCl_3$) d 7.00 (s, 1H), 3.29 (t, N_3CH_2, 2H (58%)), 2.83 (t, CH_2, 2H), 1.92-1.25 (m, CH_2, 8H), 0.94 (1, CH_3, 3H (42%)).

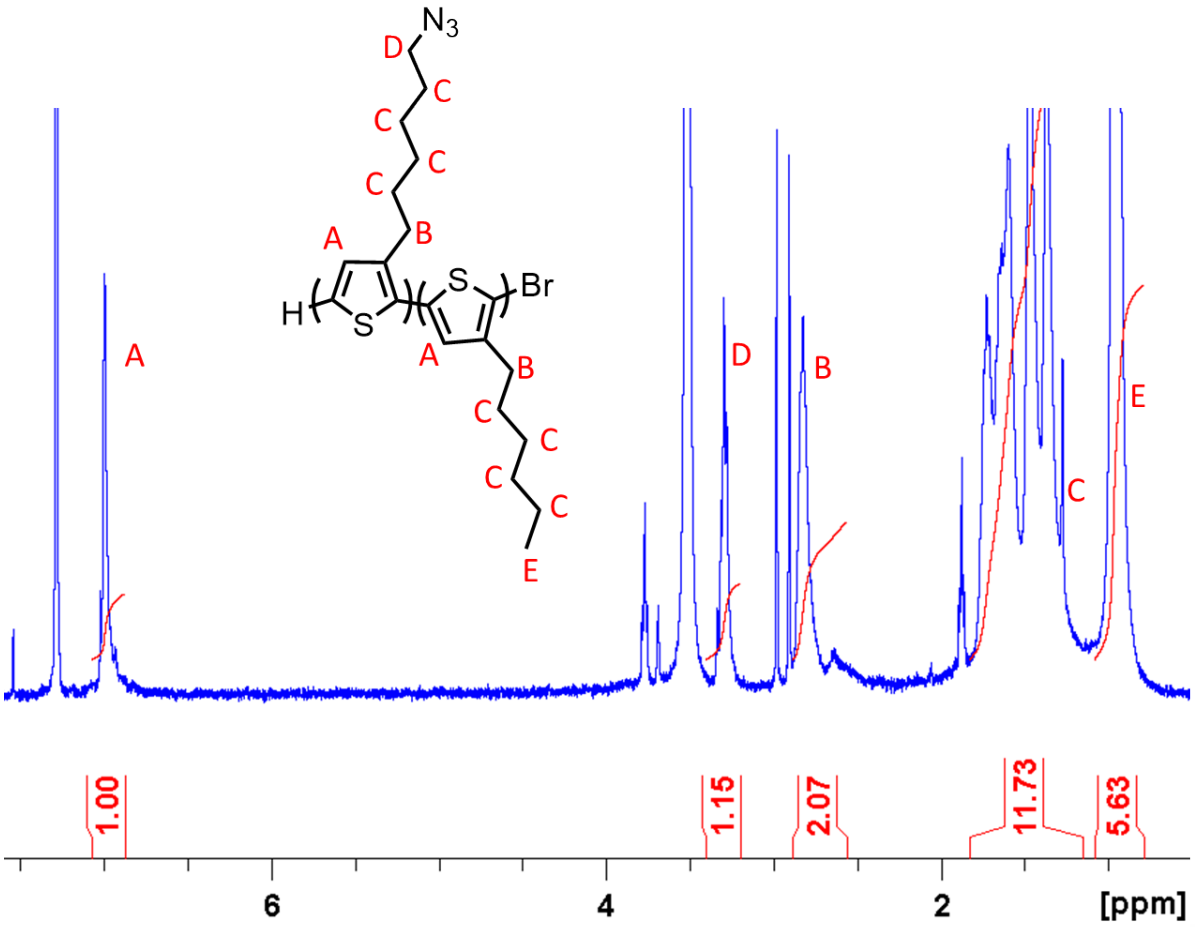

Figure S2: ^{1}H NMR spectra ($CDCl_3$) for poly(3-hexylthiophene-co-3-(azidohexyl thiophene)).

4.3 GPC/FTIR of PT Backbones

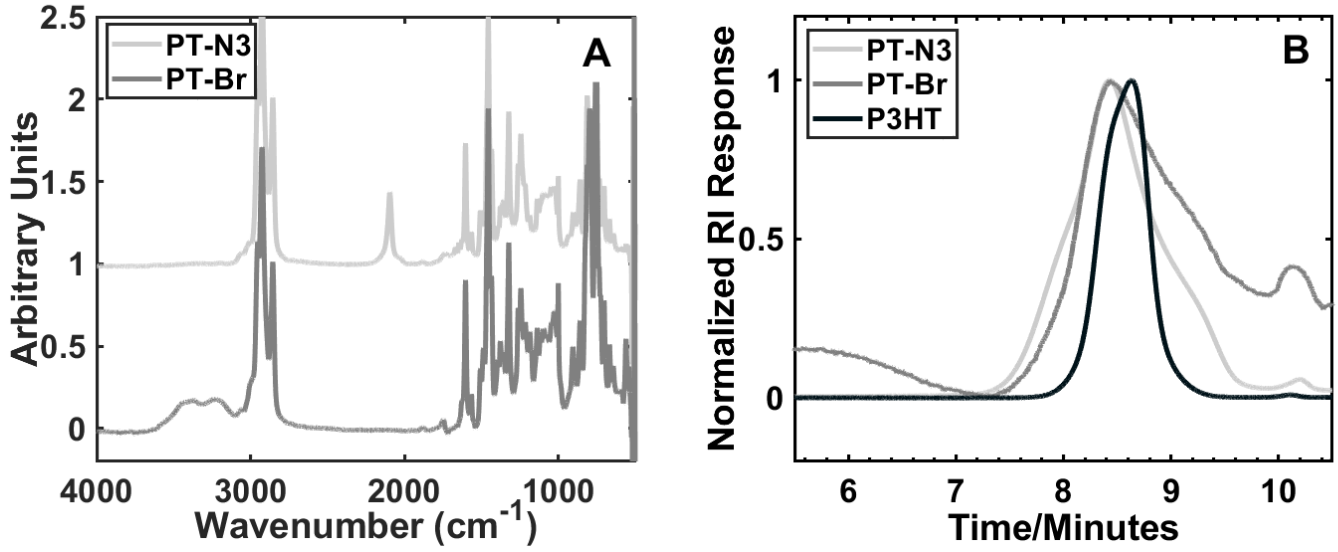

Figure S3: (a) GPC of P3HT, PT-Br, and PT-N3, (b) FTIR of PT-Br, and PT-N_3.

5 Synthetic procedure for side chains

5.1 Synthesis of P3HT-Br

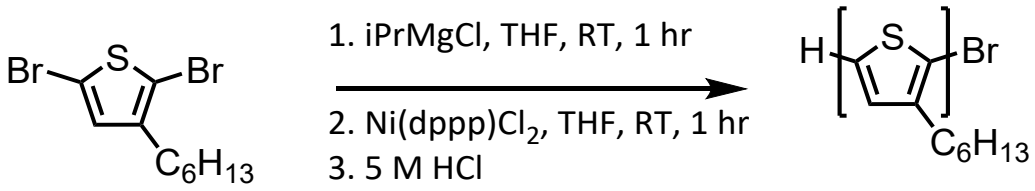

1.61 mL (7.5 mmol, 1 equiv.) 2,5-dibromo-3-hexylthiophene was added to a vacuum dried 20 mL vial with a stirr bar and dissolved in 2.6 mL THF. 3.75 mL (1 equiv.) 2 M isopropyl magnesium chloride solution in THF was added dropwise under an argon environment to the vial. The reaction was stirred for 1 hr at room temperature. A mixture of 203 mg (0.375 mmol, 0.05 equiv.) Ni(dppp)Cl2 in 44 mL THF was prepared in a 250 mL RBF. The monomer solution was added a once to the nickel solution. The reaction was stirred for 1 hour at room temperature, then quenched with 6 mL of 5 M HCl. The reaction was precipitated in methanol. The product was purified by Soxhlet extractions using methanol (12 hrs), acetone (12 hrs), hexanes (12 hrs). The hexane fraction was concentrated under reduced pressure and dried under vacuum. ^{1}H NMR (500 MHz, $CDCl_3$) d 7.00 (s, 8.5H), 2.83 (s, 14H), 2.64 (t, 1H), 2.59 (t, 1H), 1.73 (s, 16H), 1.40 (s, 48H), 0.94 (s, 24).

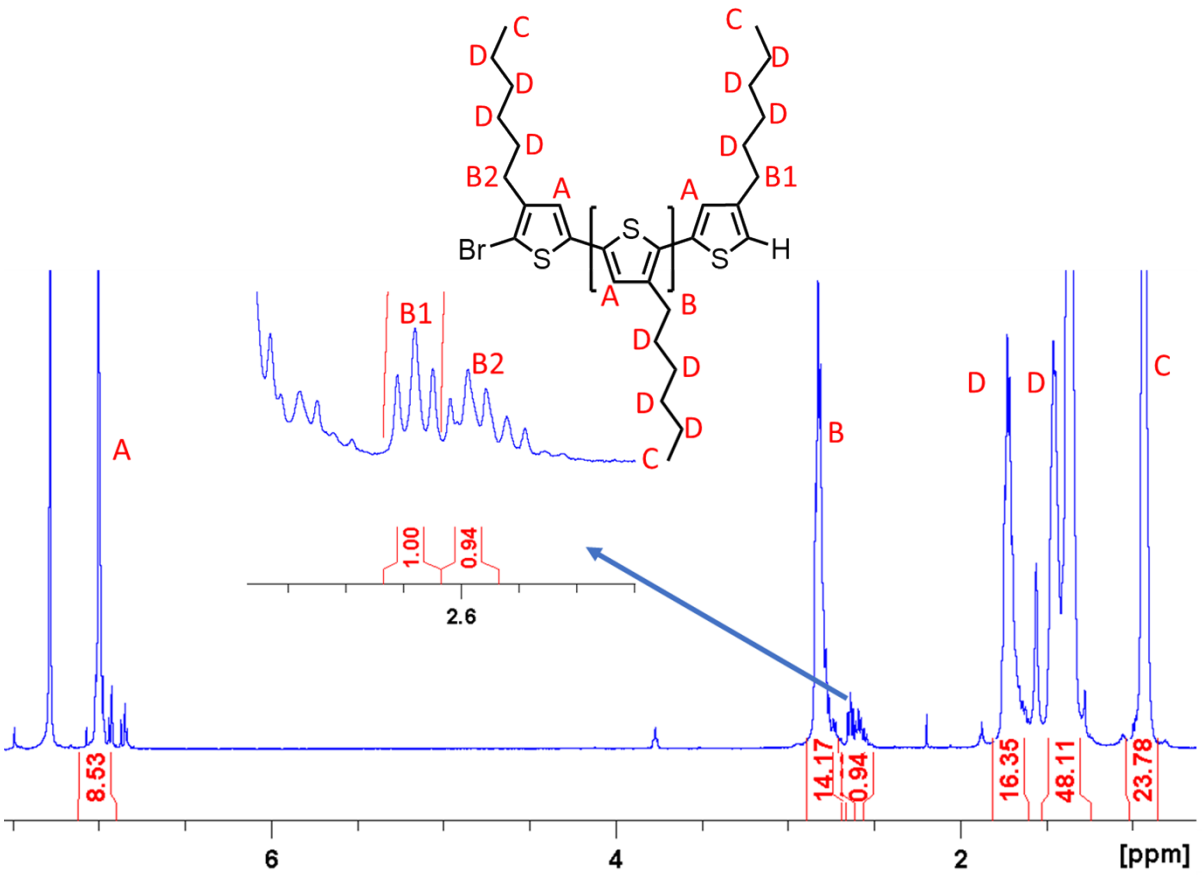

Figure S4: ^{1}H NMR spectra ($CDCl_3$) for P3HT-Br.

5.2 Synthesis of P3HT-alkyne

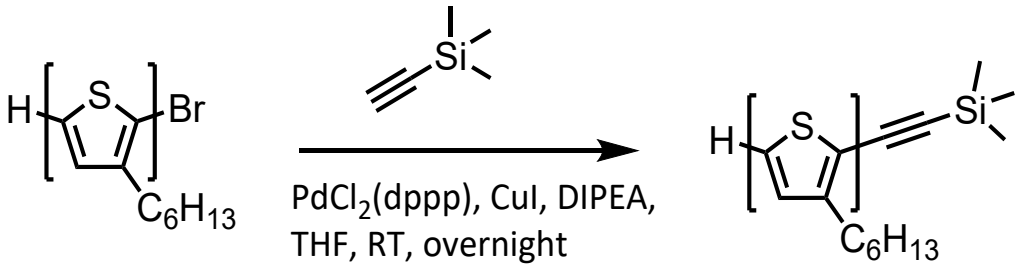

385 mg of P3HT-Br was added to a oven-dried 20 mL vial with a stirr bar. Under an argon atmosphere, 5 mL of THF and 5 mL of triethylamine was added to the vial. 213 microL (1.54 mmol, 4 equiv) trimethylsilylacetylene was added to the mixture. Then, a 500 microL solution of 75.8 mg (0.11 mmol, 0.28 equiv) Pd(PPh3)2Cl2 and 40.4 mg (0.21 mmol, 0.55 equiv) CuI was added to the reaction. The reaction was heated to 65 C overnight. The reaction was precipitated in methanol and washed with acetone, then dried under vacuum. ^{1}H NMR (500 MHz, $CDCl_3$) d 7.00 (s, 13H), 2.82 (s, 27H), 1.71 (s, 29H), 1.40 (s, 88H), 0.94 (s, 43H), 0.29 (s, 9H).

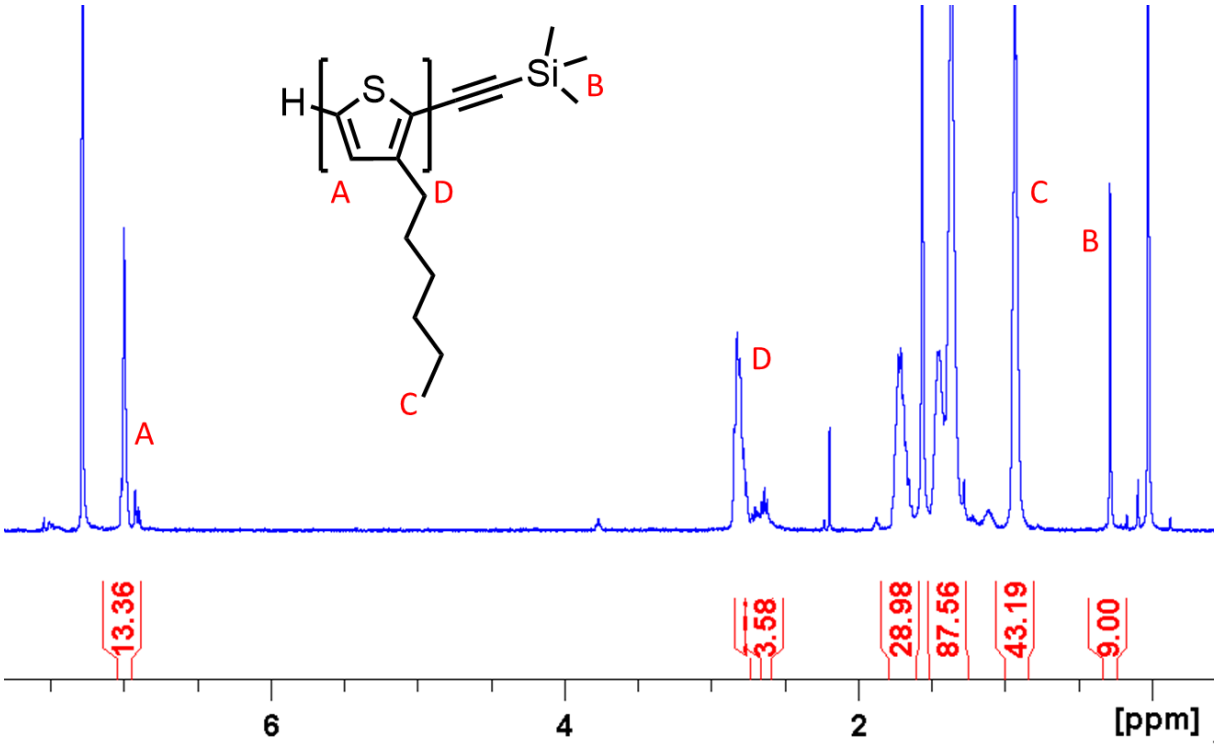

Figure S5: ^{1}H NMR spectra ($CDCl_3$) for P3HT-alkyne.

5.3 MADLI of P3HT Side Chains

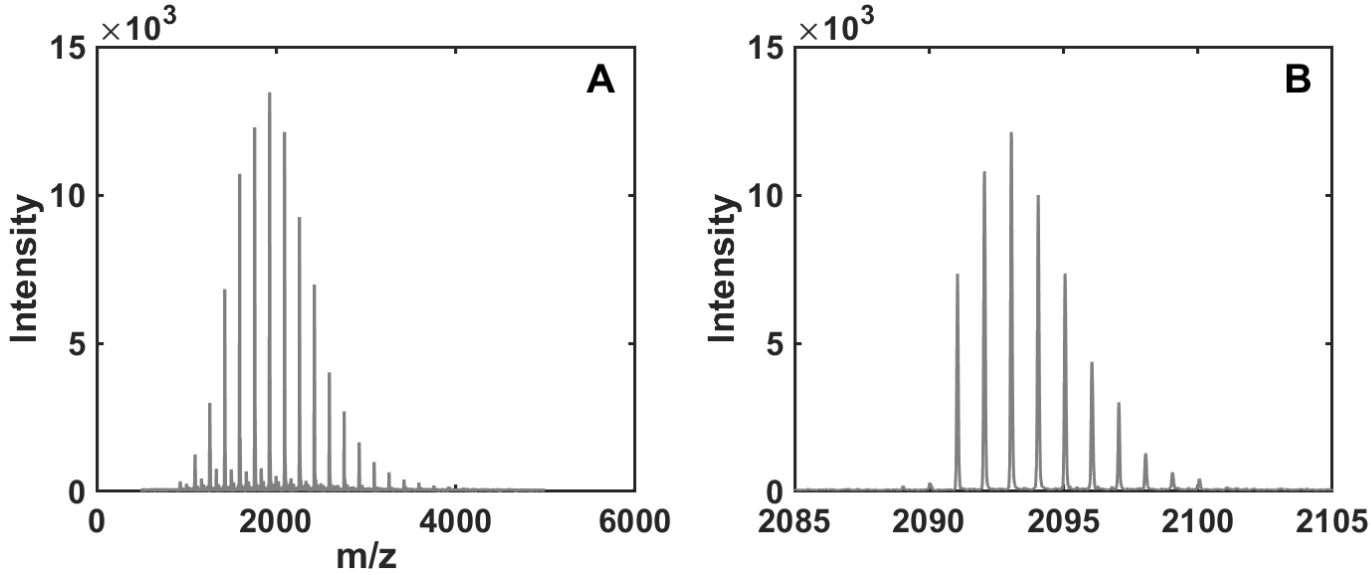

Figure S6: High-Resolution MALDIT-TOF of P3HT side chains (a) full spectrum, (b) zoomed in for isotope analysis.

5.4 Synthesis of PEO-alkyne

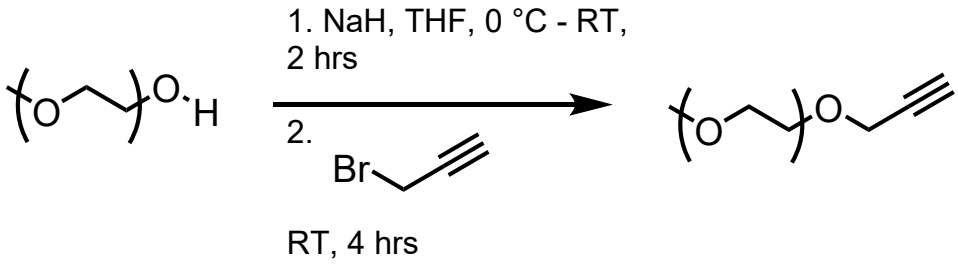

1 g (0.526 mmol, 1 equiv.) Poly(ethylene oxide) was dissolved in 15 mL THF. The mixture was cooled to 0 C, then a solution of 33.7 mg (0.842, 1.6 equiv.) sodium hydride in 5 mL THF was added dropwise. The reaction was stirred at room temperature for 2 hrs, then 102.5 microL (0.92 mmol, 1.73 equiv.) of propargyl bromide in toluene was added and the solution was stirred at room temperature for another 4 hrs. The reaction was concentrated under reduced pressure, then extracted with hexanes and washed with water. The reaction was dried with MgSO4, filtered and dried under vacuum. ^{1}H NMR (500 MHz, $CDCl_3$) d 4.24 (s, 2H), 3.67 (s, 103H), 3.41 (s, 3H), 2.45 (s, 1H).

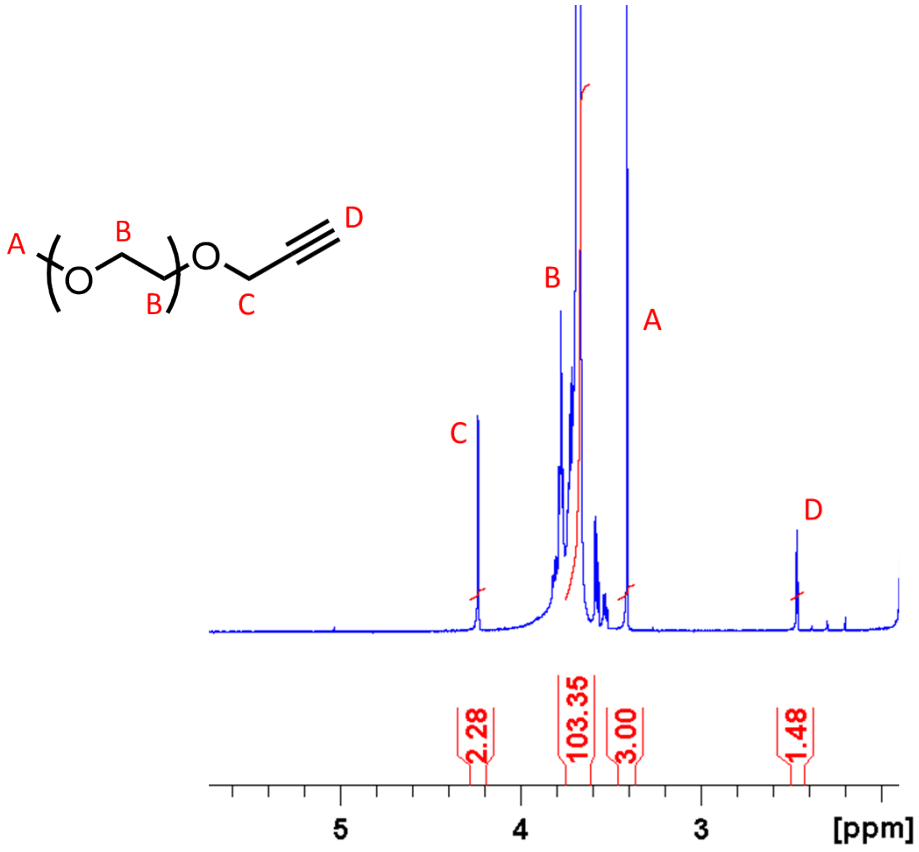

Figure S7: ^{1}H NMR spectra ($CDCl_3$) for PEO-alkyne.

5.5 Synthesis of PMMA-alkyne

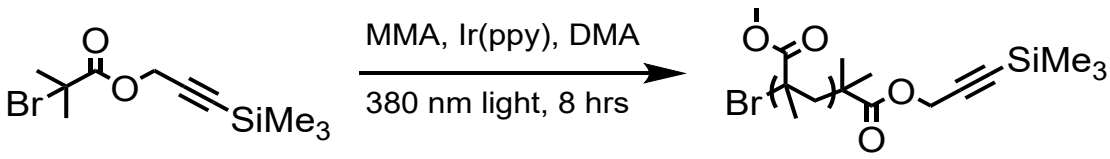

To a vacuum dried 20 mL vial with a stirr bar, 3 mL (32.0 mmol, 50 equiv) MMA was added. 14 mL of DMA and 2.1 mg (0.0032 mmol, 0.005 equiv) Ir(ppy) was added to the vial. After, 125.0 microL (0.64 mmol, 1 equiv) of 3-(1,1,1-trimethylsilyl)-2-propynyl 2-bromo-2-methylpropanoate was added to the vial. The reaction was irradiated under 380 nm light for 8 hrs. The product was precipitated in water:methanol 1:1, filtered and dried under vacuum. ^{1}H NMR (500 MHz, $CDCl_3$) d 4.65 (m, 2H), 3.62 (s, 80H), 1.92 (s, 6H), 1.04 (s, 27H), 0.88 (s, 49H), 0.20 (s, 9H).

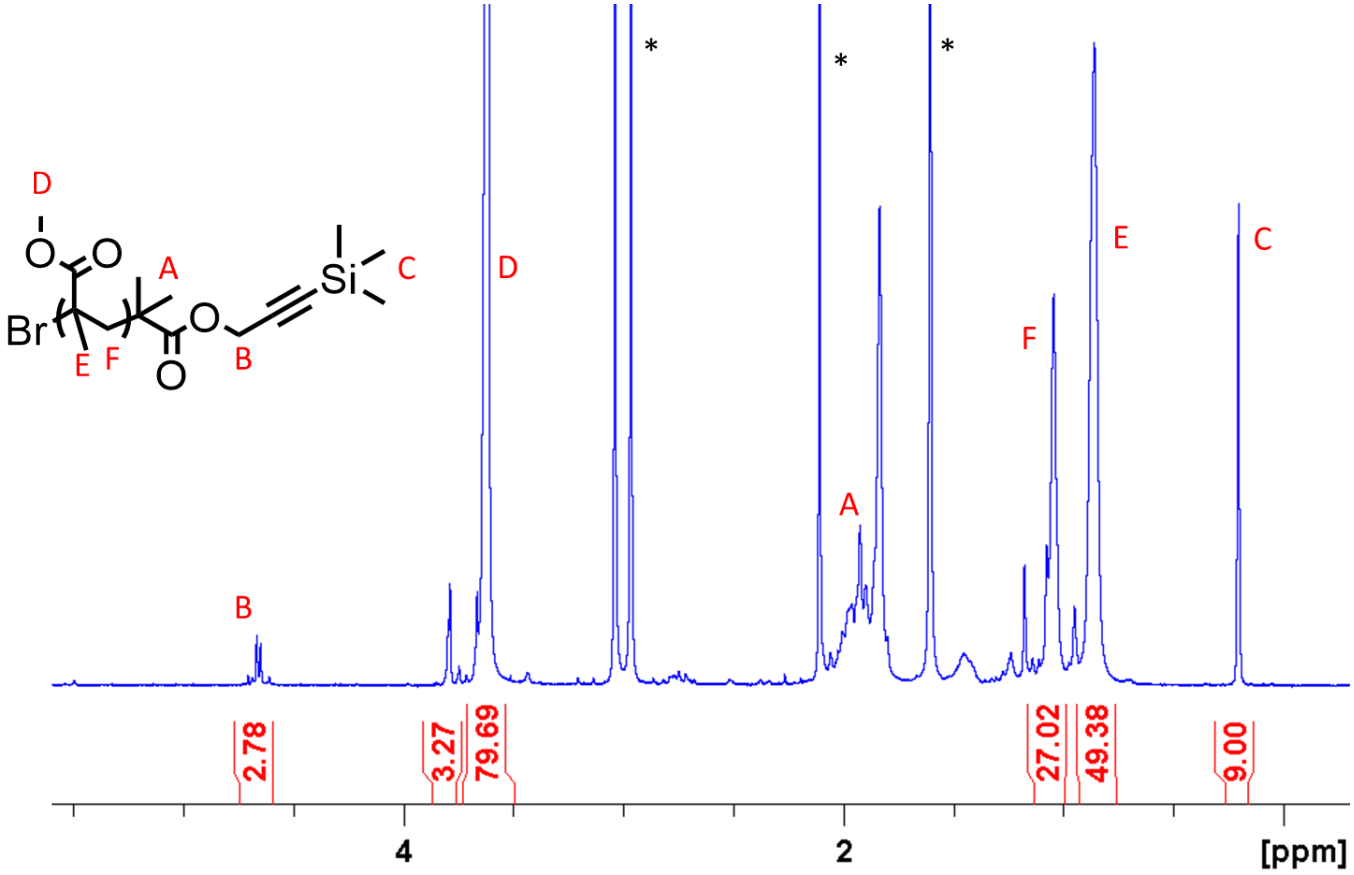

Figure S8: ^{1}H NMR spectra ($CDCl_3$) for PMMA-alkyne. * Residual DMA and water

6 Synthetic procedure for graft polymers

6.1 General procedure for grafting-to

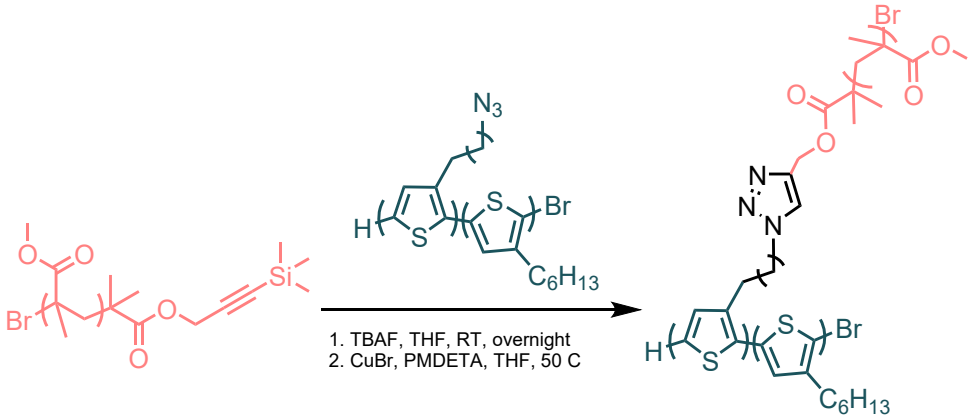

An oven dried 20 mL vial was charged with a stirr bar and PMMA-alkyne or P3HT-alkyne. The polymers were dissolved in THF and TBAF was added. The mixtures were stirred overnight at room temperature to deprotect the alkynes. This step was skipped by the PEO-alkyne polymers. The azide containing backbones were added to the polymer mixture, then 1 equivalent of a CuBr/PMDETA catalyst solution was added to the mixture. The reaction was stirred at 50 C overnight. The polymers were then precipitated in methanol/water mixtures.

6.2 Synthesis of PT-*graft*-PEO:

120 mg of PEO-alkyne was added to a 20 mL oven dried vial and dissolved in 10 mL THF. 19.2 mg PT-N3 was added to the vial and 123 microL of the catalyst solution (60 mg CuBr, 87 microL PMDETA, 2 mL THF) was added. The reaction was stirred overnight at room temperature. The product was precipitated in methanol:water 1:1. ^{1}H NMR (500 MHz, $CDCl_3$) d 7.57 (s, triazole-H), 7.00 (s, 1H, thiophene-H), 4.69 (s, 2H), 4.37 (s, 2H), 3.69 (s, 164H), 2.81 (s, 1H), 1.59 (s, 44H), 1.28 (s, 8.5H), 0.92 (s, 3H).

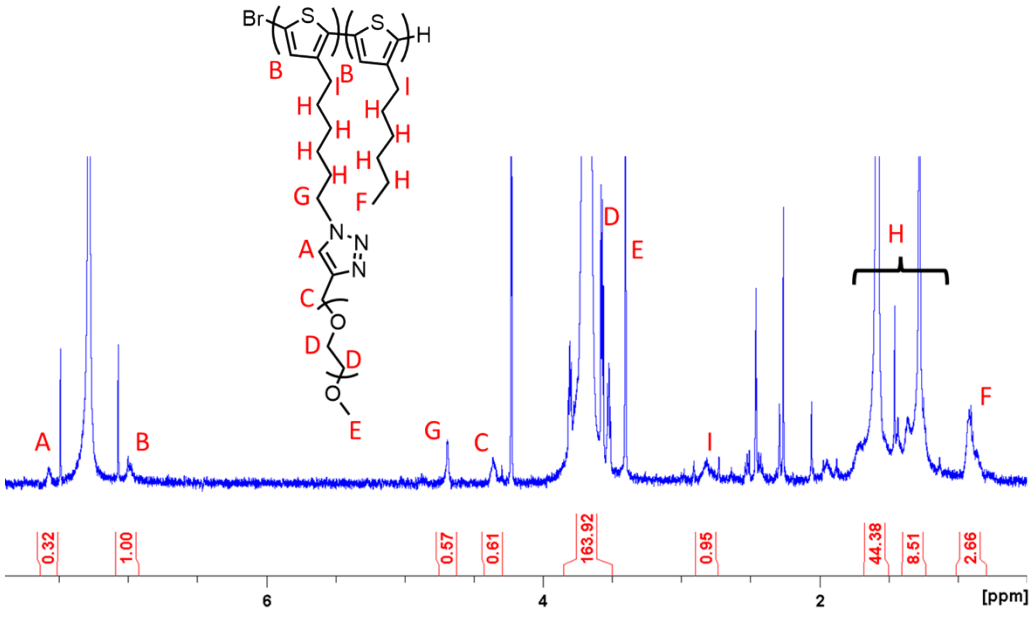

Figure S9: ^{1}H NMR spectra ($CDCl_3$) for PT-*g*-PEO.

6.3 Synthesis of PT-*graft*-P3HT:

100 mg of P3HT-alkyne was added to a 20 mL oven dried vial and dissolved in 10 mL THF. 0.5 mL 1M TBAF was added to the mixture and stirred overnight at room temperature. 19.2 mg PT-N3 was added to the vial and 123 microL of the catalyst solution was added. The reaction was stirred overnight at room temperature. The product was precipitated in methanol, and purified by Soxlet extraction in hexanes. ^{1}H NMR (500 MHz, $CDCl_3$) d 7.57 (s), 6.99 (s, 1H), 4.40 (s), 2.81 (s, 2H), 1.89-0.98 (m, 24H), 0.92 (s, 3H).

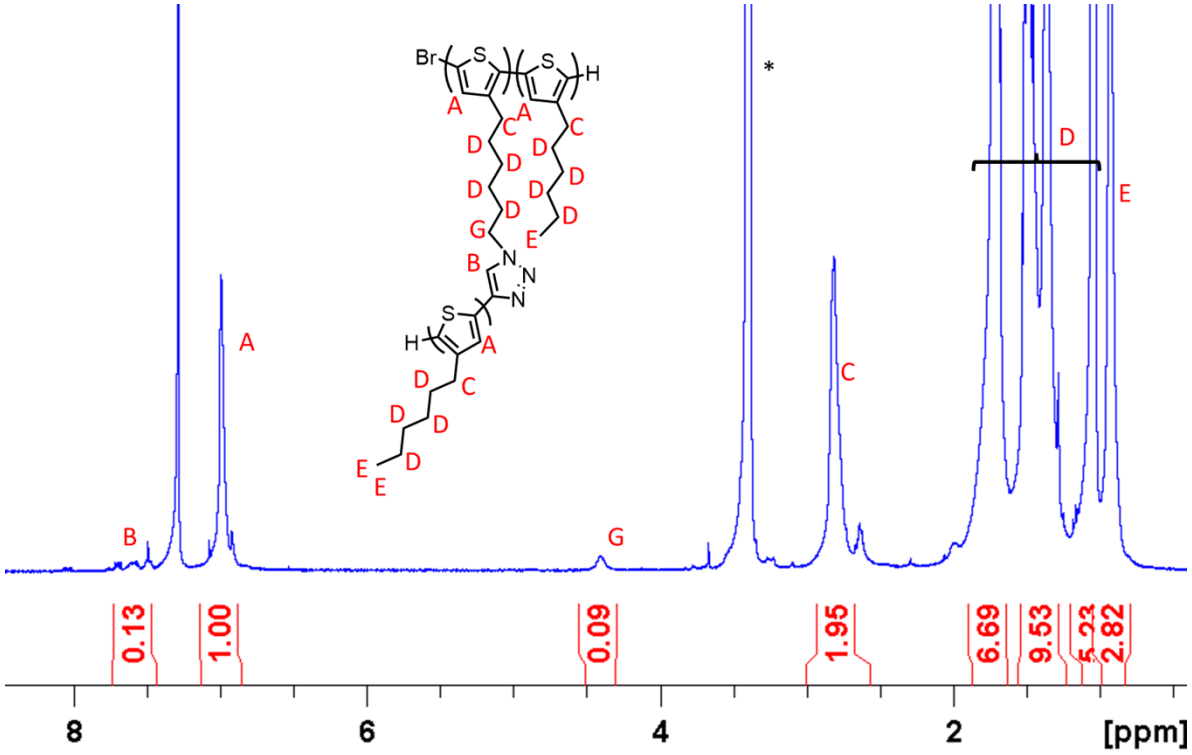

Figure S10: ^{1}H NMR spectra ($CDCl_3$) for PT-*g*-P3HT.

6.4 Synthesis of PT-graft-PMMA:

100 mg of PMMA-alkyne was added to a 20 mL oven dried vial and dissolved in 10 mL THF. 0.4 mL 1M TBAF was added to the mixture and stirred overnight at room temperature. 19.2 mg PT-N3 was added to the vial and 123 microL of the catalyst solution was added. The reaction was stirred overnight at room temperature. The product was precipitated in methanol, and purified by Soxlet extraction in methanol. ^{1}H NMR (500 MHz, $CDCl_3$) d 7.61 (s, 0.5H), 7.00 (s, 1H), 5.20 (s, 1H), 4.36 (s, 1H), 3.66 (s, 47H), 2.81 (s, 2H), 1.89 (s, 23H), 1.78-0.97 (m, 78H), 0.87 (s, 24H).

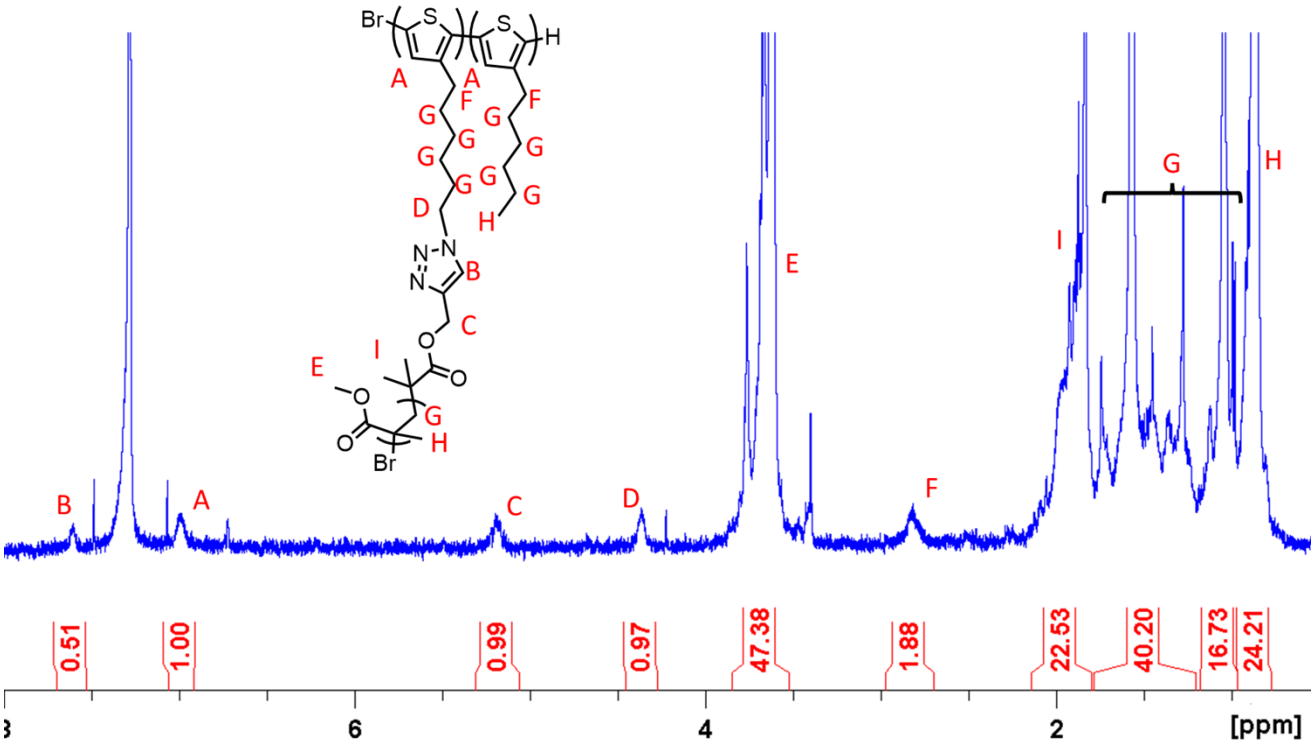

Figure S11: ^{1}H NMR spectra ($CDCl_3$) for PT-*g*-PMMA.

7 Calculations of NMR molecular weights, mol% SC, w% SC, grafting efficiency

7.1 Side Chain molecular weight from end group analysis:

From normalizing to a peak on the polymer end group:

$Ratio * M_{n,m_{sc}} + MW_{endgroup} = M_{n,SC,NMR}$

Table S1: End group analysis of side chains.

Polymer	Monomer Molecular weight, $M_{n,m_{sc}}$ (g/mol)	End group MW (g/mol)	DP from ratio of EG to monomer	$M_{n,SC,NMR}\left(\frac{g}{mol}\right)$
PMMA-alkyne	100.12	265.22	80/3	2900
PEO-alkyne	56.06	72.11	103/4	1500
P3HT-alkyne	166.28	98.22	13.4	2300

7.2 Degree of polymerization from GPC for backbone:

$Ratio * M_{n,m_1} + (1 - Ratio) * M_{n,m_2} = Effective\ M_{n,monomer}$

$(M_{n,SEC} - M_{Endgroup})/Effective\ M_{n,monomer} = DP$

Table S2: Degree of polymerization of P3HT, PT-Br, PT-N_3.

Polymer	Monomer 1 molecular weight, M_{n,m_1}	M_{n,m_2}	$MW_{Endgroup}$	Ratio monomer1 / monomer2*	$M_{n,SEC}$	Effective $M_{n,monomer}$	DP
PT-Br	166.28	245.18	80.91	0.42	3900	212.04	18
PT-N3	166.28	207.29	43.03	0.42	6900	189.86	36
P3HT	166.28	-	80.91	-	6500	166.28	39

*From NMR

7.3 Graft molecular weight from NMR:

$Ratio * DP_{backbone} = N_{SC}$

$N_{SC} * M_{n,m_{sc}} + MW_{backbone} = M_{n,NMR}$

Table S3: M_n of grafted polymers.

Polymer	$M_{n,m_{sc}}$ (g/mol)	Ratio of triazole to backbone	$M_{n,NMR}\left(\frac{g}{mol}\right)$	Number of side chains per backbone, N_{SC}
PT-*g*-PMMA	100.12	0.51	59100	18
PT-*g*-PEO	56.06	0.32	24150	11.5
PT-*g*-P3HT	166.28	1/0.17/21= 0.28	29900	10

^: calculated from peak G integration (Figure S12), where 0.09 corresponds to molar percent of N3 backbone monomers in all thiophene monomers and using the ratio 0.58 mol% N3 backbone monomers, therefor 0.17 mol% backbone monomers

7.4 Mol% Side Chains, Mass% Side Chains, Aromaticity%, grafting efficiency

$$\frac{M_{n,NMR,graft}}{N_{SC} * M_{n,m_{sc}}} = w_{SC}$$

$$w_{aroma,BB} * (1 - w_{SC}) + w_{SC} * w_{aroma,SC} = w_{aroma,graft}$$

$$w_{aroma,BB} = \frac{M_{n,atoms\ in\ aromatic\ rings}}{Effective\ M_{n,mononer}} = \frac{81.12}{226.1} = 0.36$$

$$w_{aroma,SC} = \frac{M_{n,atoms\ in\ aromatic\ rings}}{M_{n,m_{sc}}} = \frac{81.18}{166.28} = 0.49\ Only\ applies\ to\ P3HT\ SCs$$

$$N_{SC}/DP_{backbone} = \varepsilon_{grafting}$$

Table S4: Weight percent and aromatic percent calculations for grafted polymers.

Polymer	wt% side chains, w_{SC}	wt% aromatics $w_{aroma,graft}$	Grafting efficiency, $\varepsilon_{grafting}$
PT-*g*-PMMA	88.3	4.3	0.86
PT-*g*-PEO	71.4	10.4	0.55
PT-*g*-P3HT	76.9	39.0	0.48

7.5 Summary of calculated values from NMR and GPC analysis

Table S5: Summary of calculated values for chemical composition.

polymer	$M_{n,\ SEC,\ THF}$ (g mol^{-1})	$D_{SEC,\ THF}$	$M_{n,\ SEC,\ CB}$ (g mol^{-1})	$D_{SEC,\ CB}$	DP	$M_{n,\ NMR}$ (g mol^{-1})	wt% side chains	wt% aromatics	Grafting efficiency
P3HT-alkyne	3000	1.15	5800	1.20	13^	2300	100	49	-
PEO-alkyne	2100	1.04			26^	1500	100	0	-
PMMA-alkyne	1700	1.03			27^	2900	100	0	-
PT-Br	3900	2.56			18#	-	0	38	-
PT-N3	5500	2.33	6900	2.37	36#	-	0	36	-
P3HT	6500	1.25			39#	-	0	49	-
PT-*g*-P3HT	16500	1.80	29000	3.36	-	29700	77	39.0	0.48
PT-*g*-PEO	16300	1.42			-	46900	71	10.4	0.55
PT-*g*-PMMA	24400	1.58	24000	1.75	-	34300	88	4.3	0.48

*D: Dispersity; DP: Degree of polymerization; ^ calculated from NMR Mn; # calculated from SEC MW

8 Mass Absorptivity calculation plots for chloroform solutions

8.1 Linear fit of absorbance vs. concentration at the max wavelength for mass absorptivity

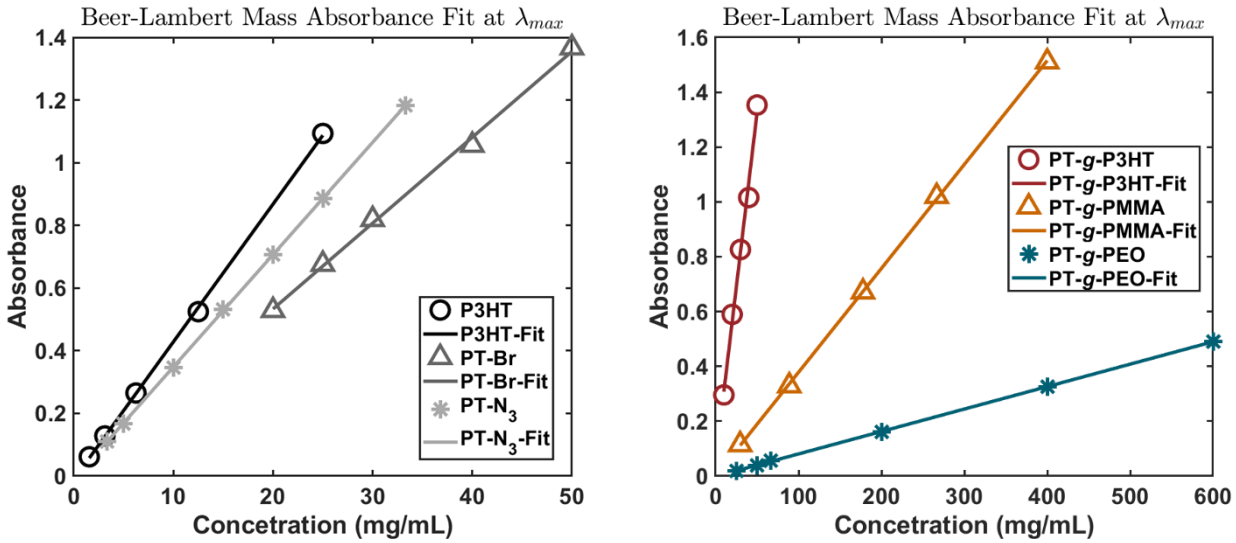

Figure S12: Representative linear fit of absorbance vs. concentration at λ_{max} for use in calculating mass absorptivity with Beer-Lambert Law for (a) P3HT, PT-Br, and PT-N_3 (b) PT-*g*-P3HT, PT-*g*-PMMA, and PT-*g*-PEO in chloroform.

8.2 P3HT

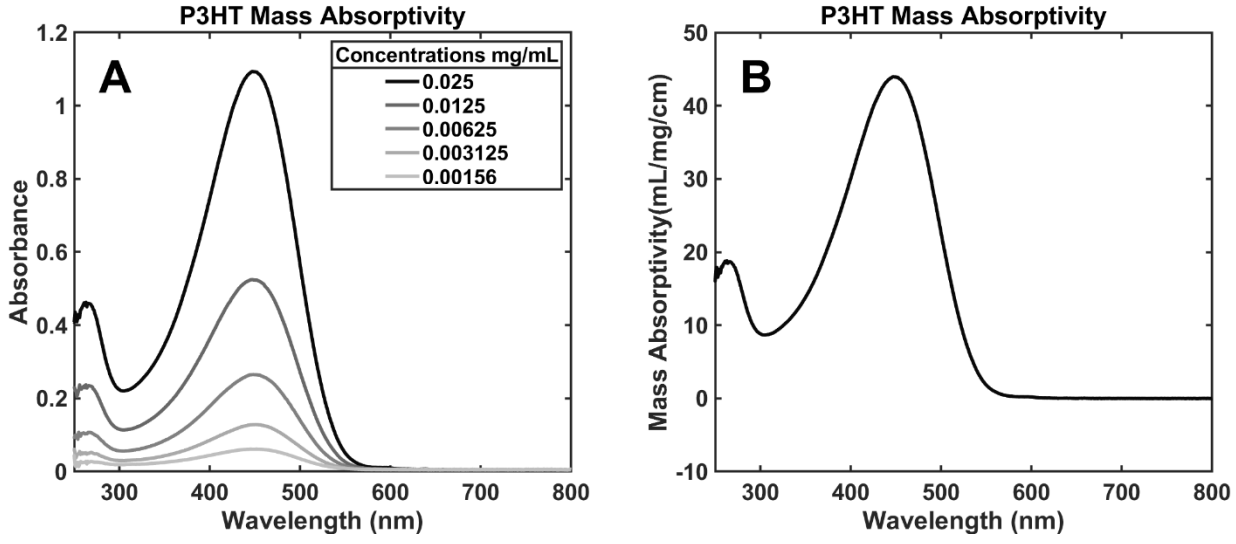

Figure S13: (a) Raw absorption curves for P3HT, (b) mass absorptivity of P3HT.

8.3 PT-Br

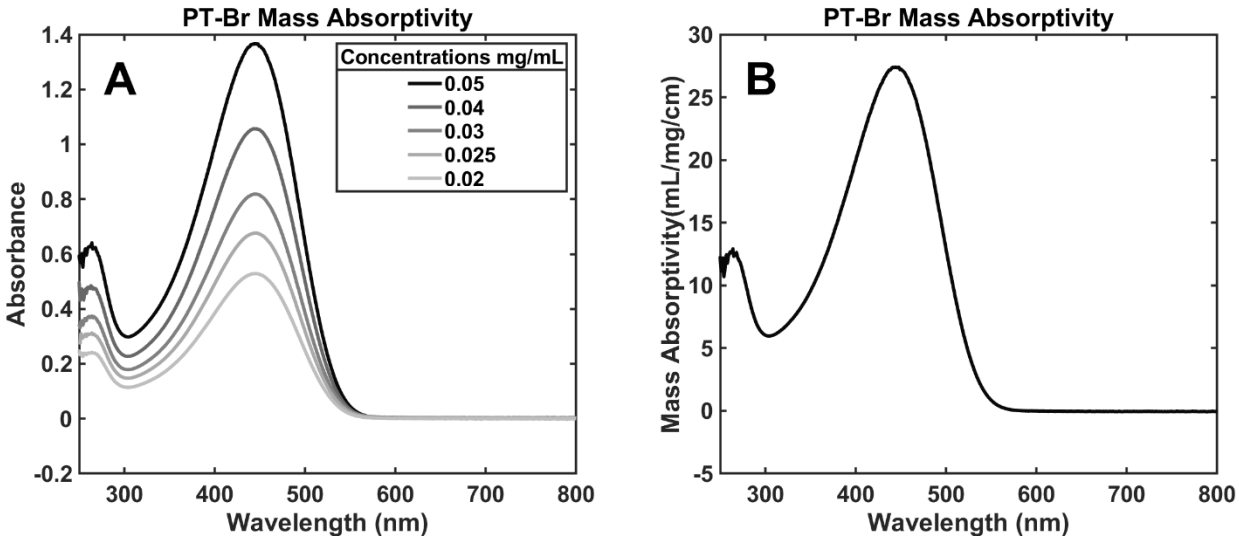

Figure S14: (a) Raw absorption curves for PT-Br, (b) mass absorptivity of PT-Br.

8.4 PT-N_3

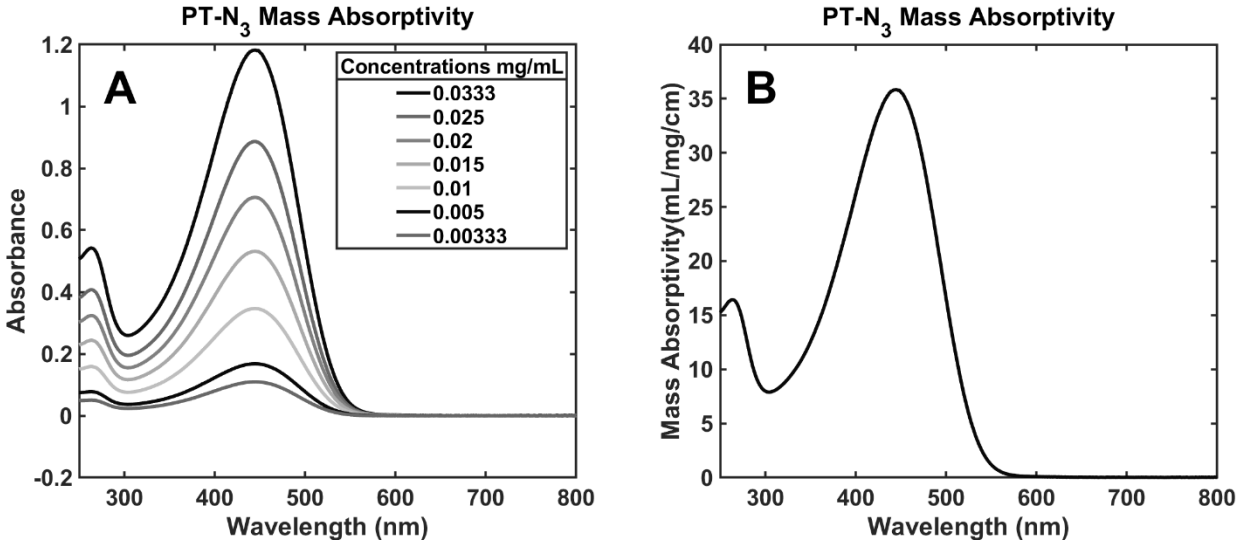

Figure S15: (a) Raw absorption curves for PT-N_3, (b) mass absorptivity of PT-N_3.

8.5 PT-*g*-P3HT

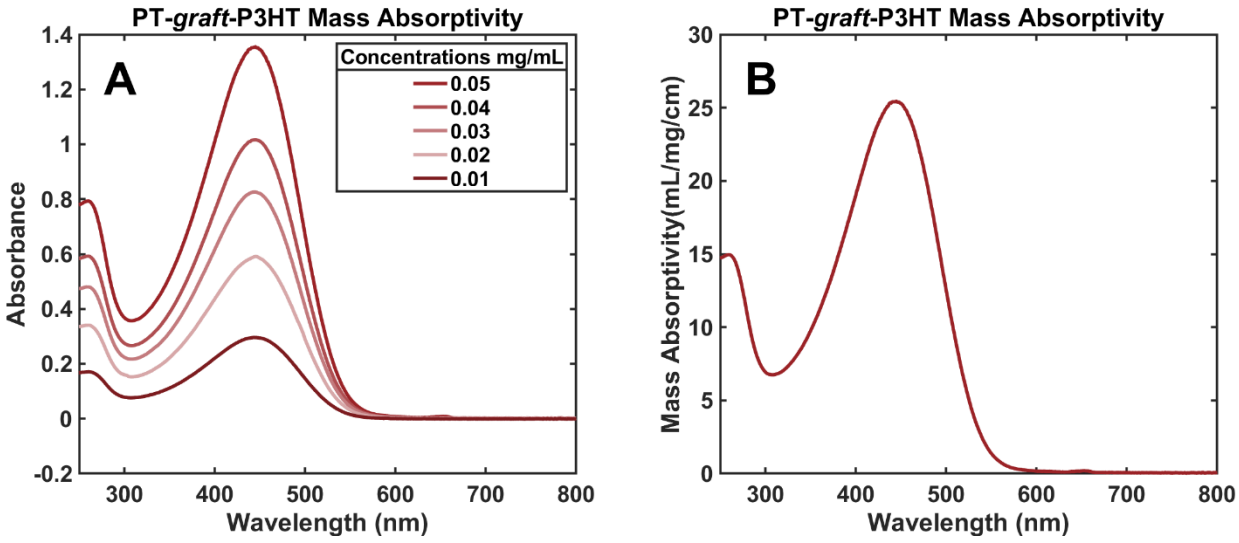

Figure S16: (a) Raw absorption curves for P3HT, (b) mass absorptivity of P3HT.

8.6 PT-*g*-PMMA

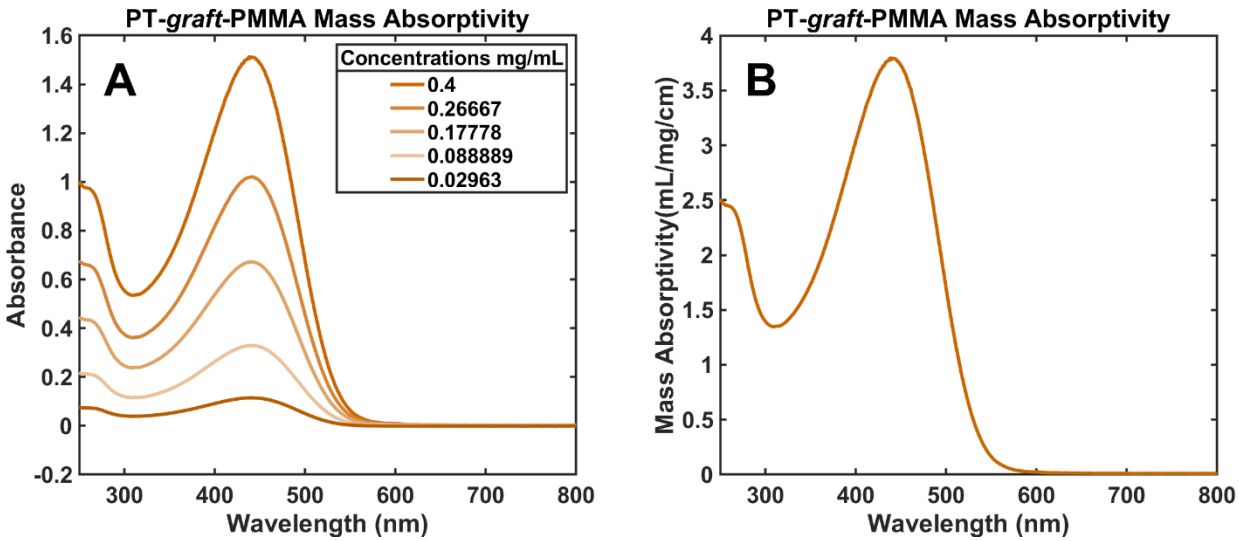

Figure S17: (a) Raw absorption curves for P3HT, (b) mass absorptivity of P3HT.

8.7 PT-*g*-PEO

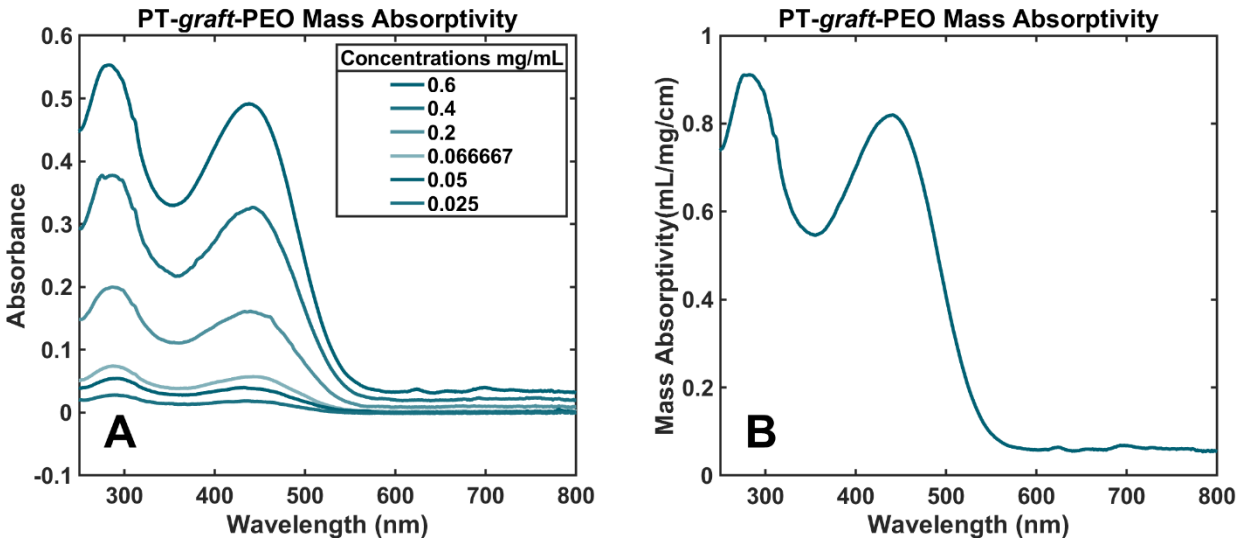

Figure S18:(a) Raw absorption curves for P3HT, (b) mass absorptivity of P3HT.

9 Normalized UV-vis absorbance and fluorescence spectra in chloroform

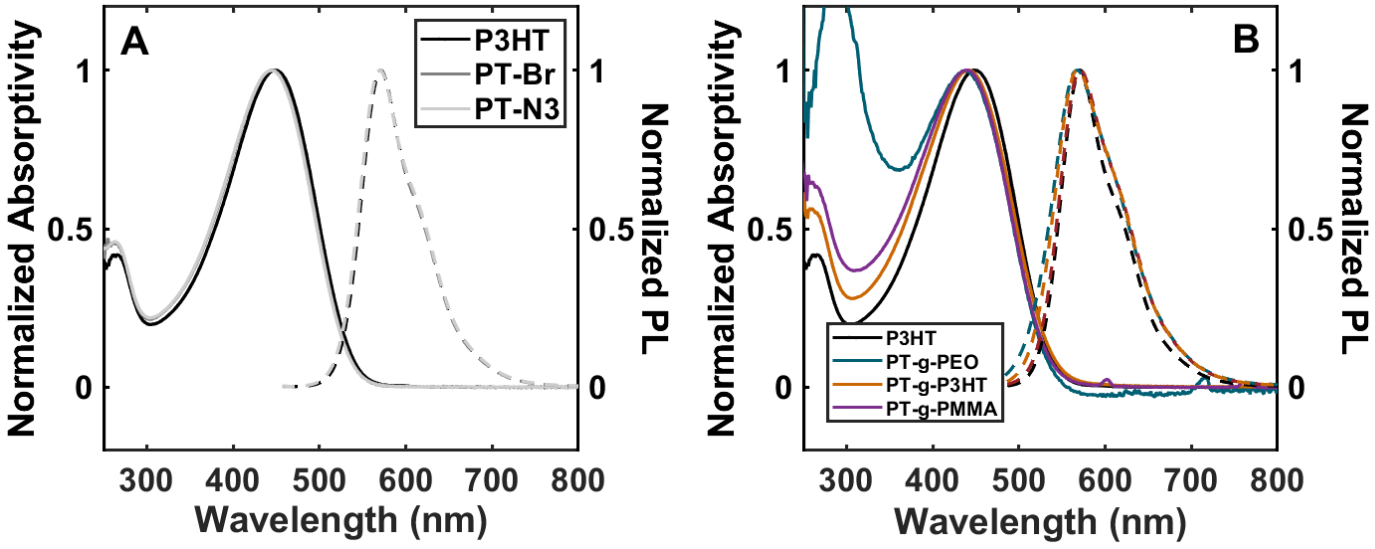

Figure S19: Normalized absorbance spectra in chloroform (a) P3HT, PT-Br, PT-N3, (b) P3HT, PT-g-PEO, PT-g-PMMA, PT-g-P3HT.

10 Quantum Yield Calculation Plots for chloroform solutions

10.1 P3HT

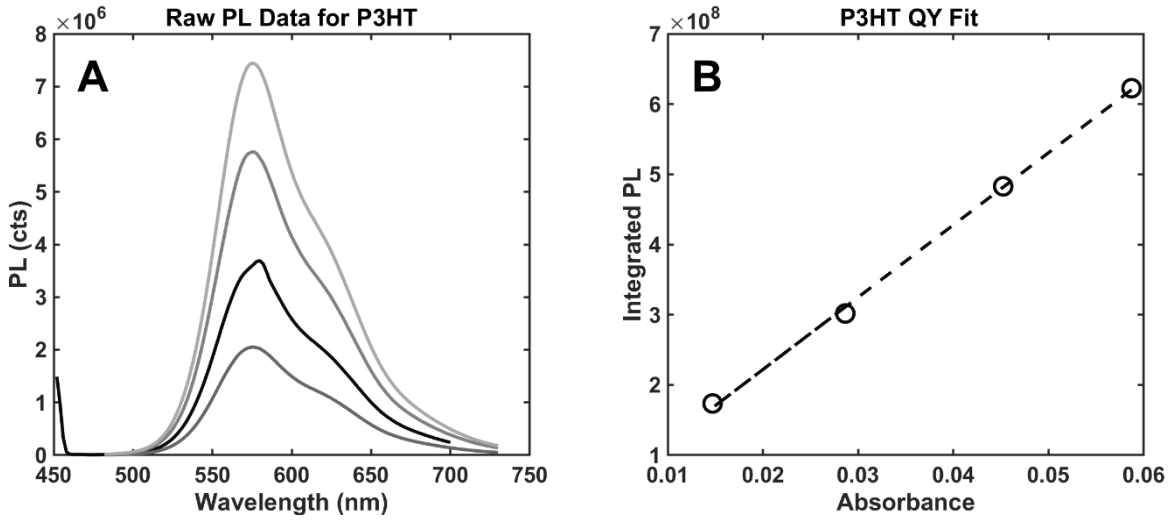

Figure S20: (a) Raw emission curves for P3HT with excitation at 450 nm, (b) integrated fluorescence vs absorbance for P3HT.

10.2 PT-*g*-P3HT

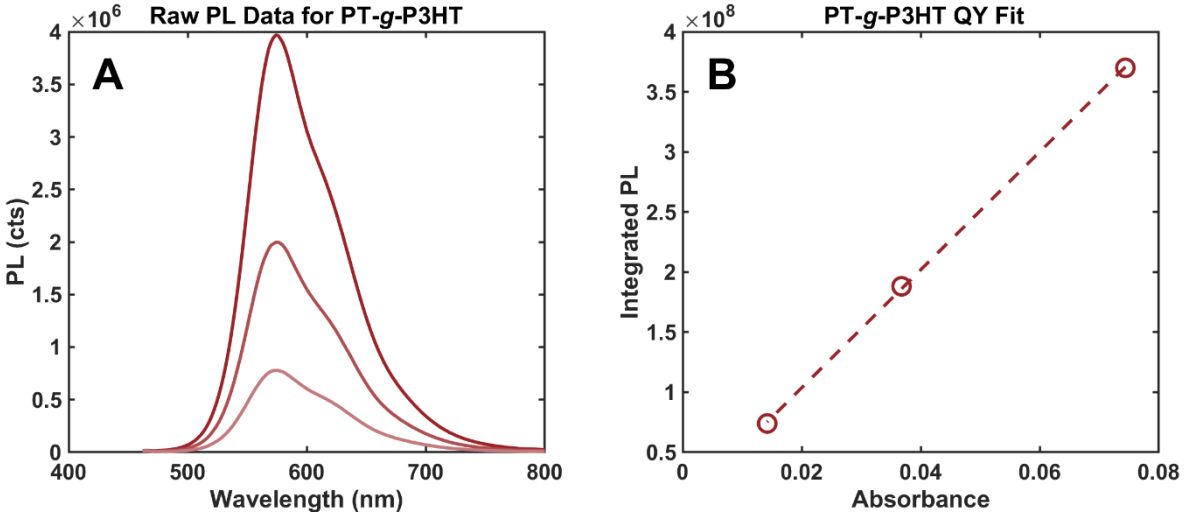

Figure S21: (a) Raw emission curves for PT-g-P3HT with excitation at 450 nm, (b) Integrated fluorescence vs absorbance for PT-g-P3HT.

10.3 PT-*g*-PMMA

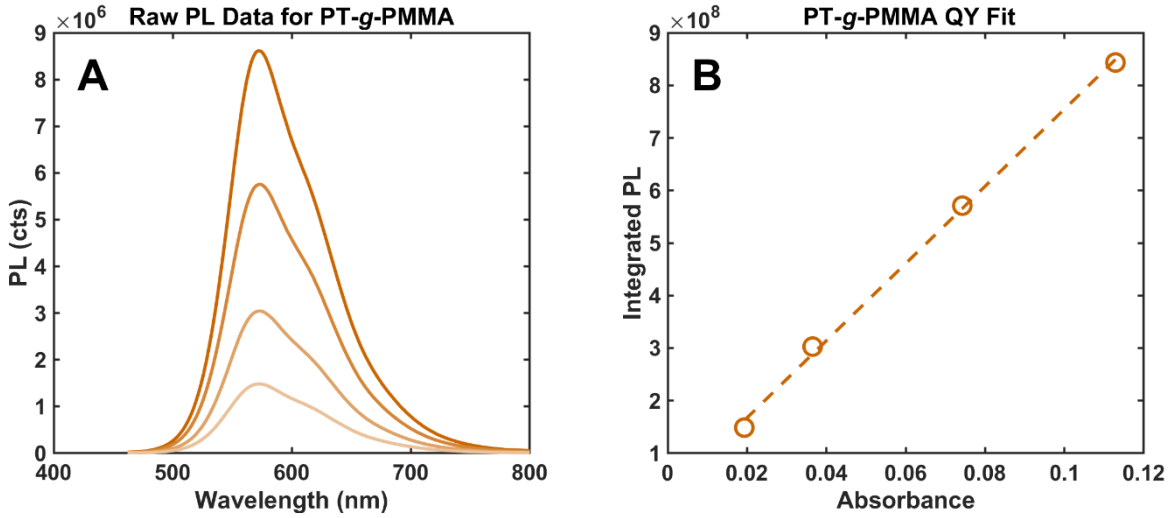

Figure S22: (a) Raw emission curves for PT-g-PMMA with excitation at 450 nm, (b) Integrated fluorescence vs absorbance for PT-g-PMMA.

10.4 PT-*g*-PEO

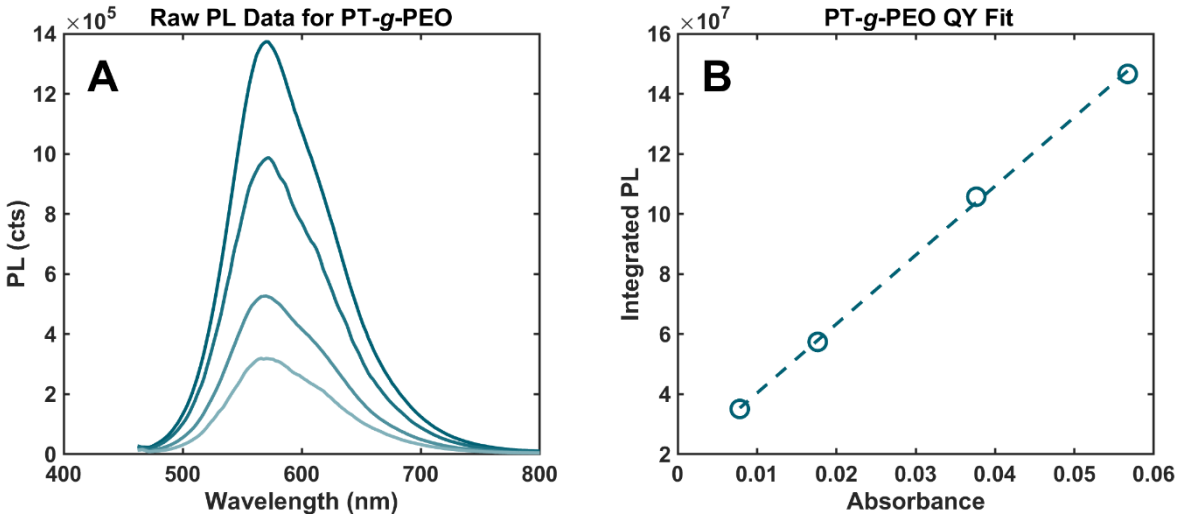

Figure S23: (a) Raw emission curves for PT-g-PEO with excitation at 450 nm, (b) Integrated fluorescence vs absorbance for PT-g-PEO.

11 Nanoparticle pictures

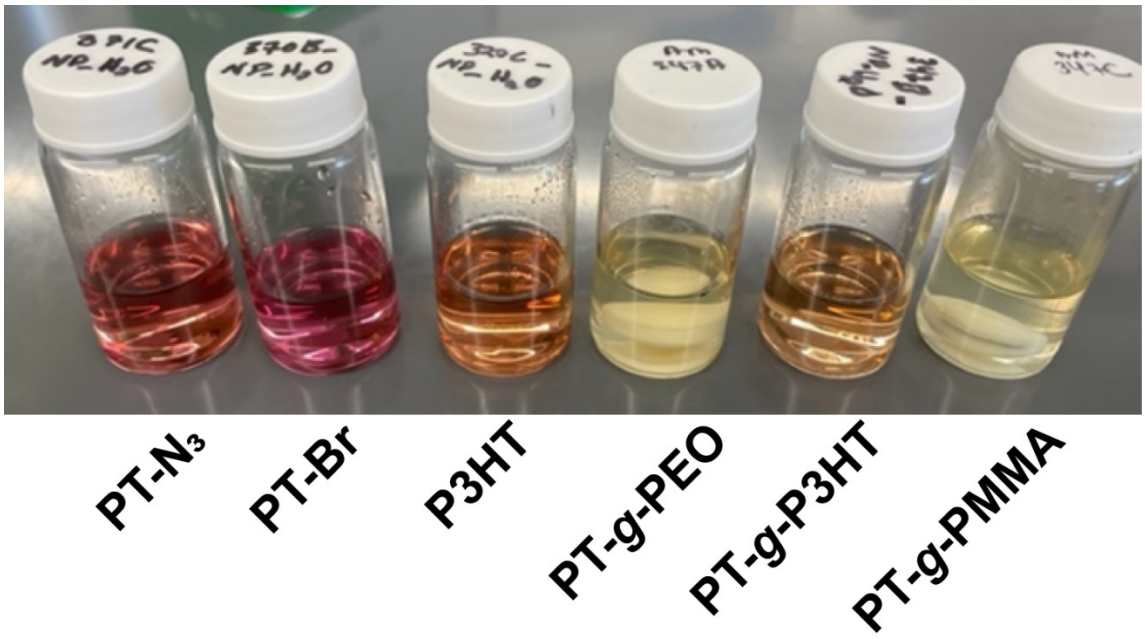

Figure S24: Physical pictures of nanoparticles in aqueous media.

12 DLS Histograms of 3 independent runs

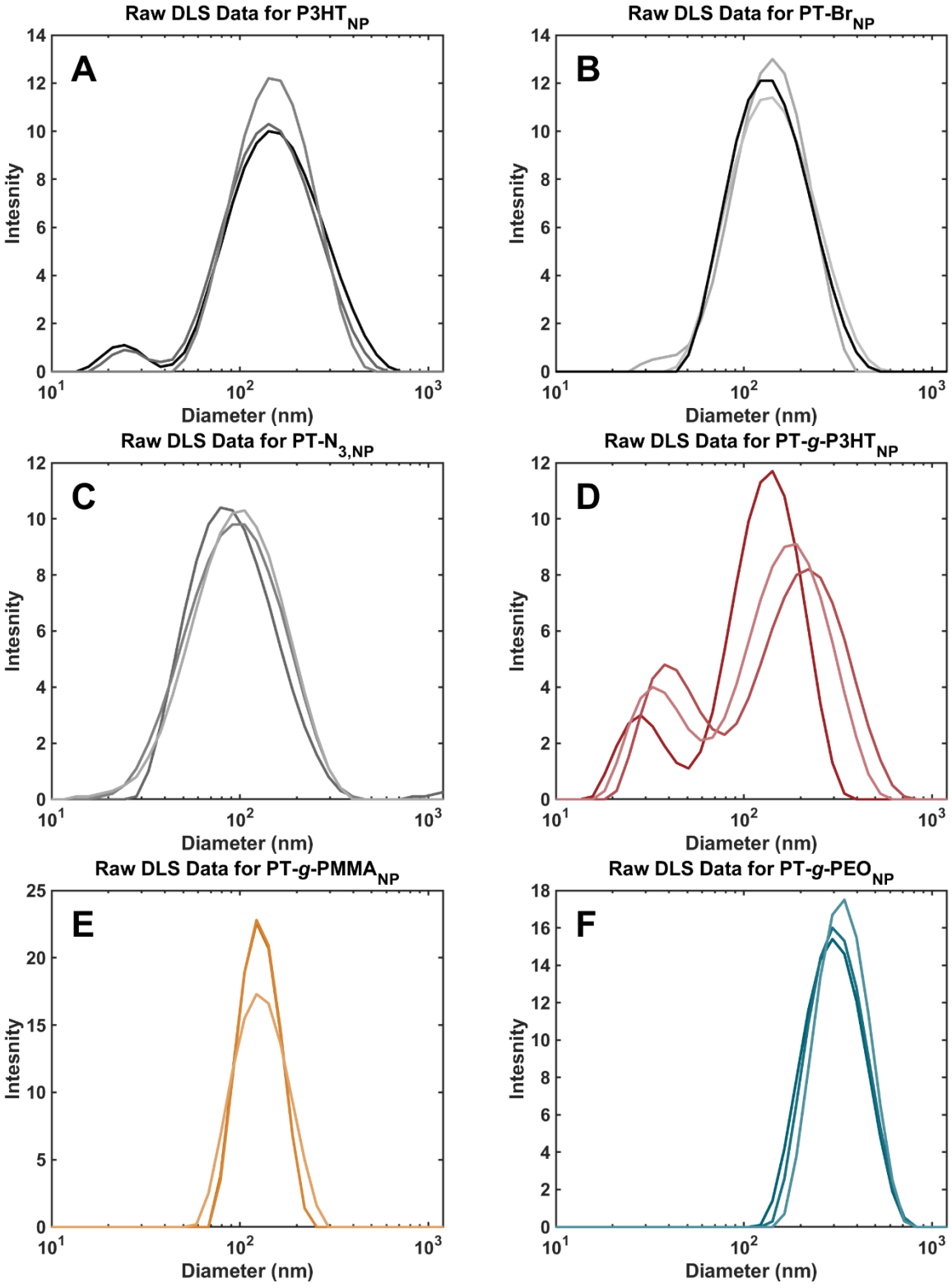

Figure S25: DLS histograms for 3 independent measurements of (a) P3HT, (b) PT-Br, (c) PT-N_3, (d) PT-*g*-P3HT, (e) PT-*g*-PMMA, and (f) PT-*g*-PEO.

13 Mass Absorptivity calculation plots for nanoparticle solutions

13.1 Linear fit of absorbance vs. concentration at the max wavelength for mass absorptivity

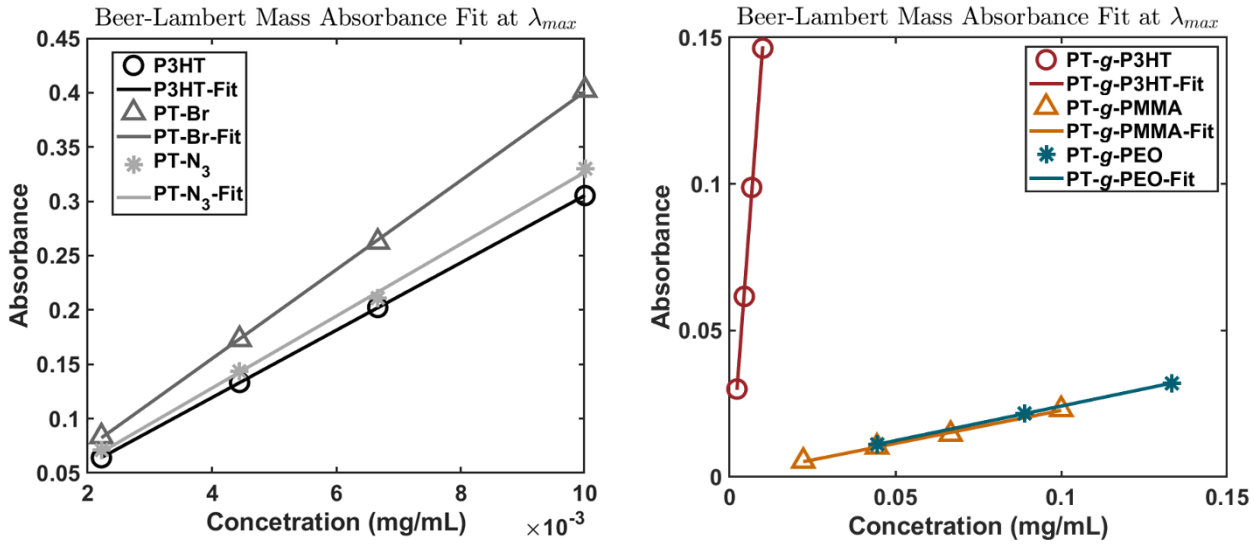

Figure S26: Representative linear fit of absorbance vs. concentration at λ_{max} for use in calculating mass absorptivity with Beer-Lambert Law for (a) P3HT, PT-Br, and PT-N_3 (b) PT-*g*-P3HT, PT-*g*-PMMA, and PT-*g*-PEO in water.

13.2 P3HT

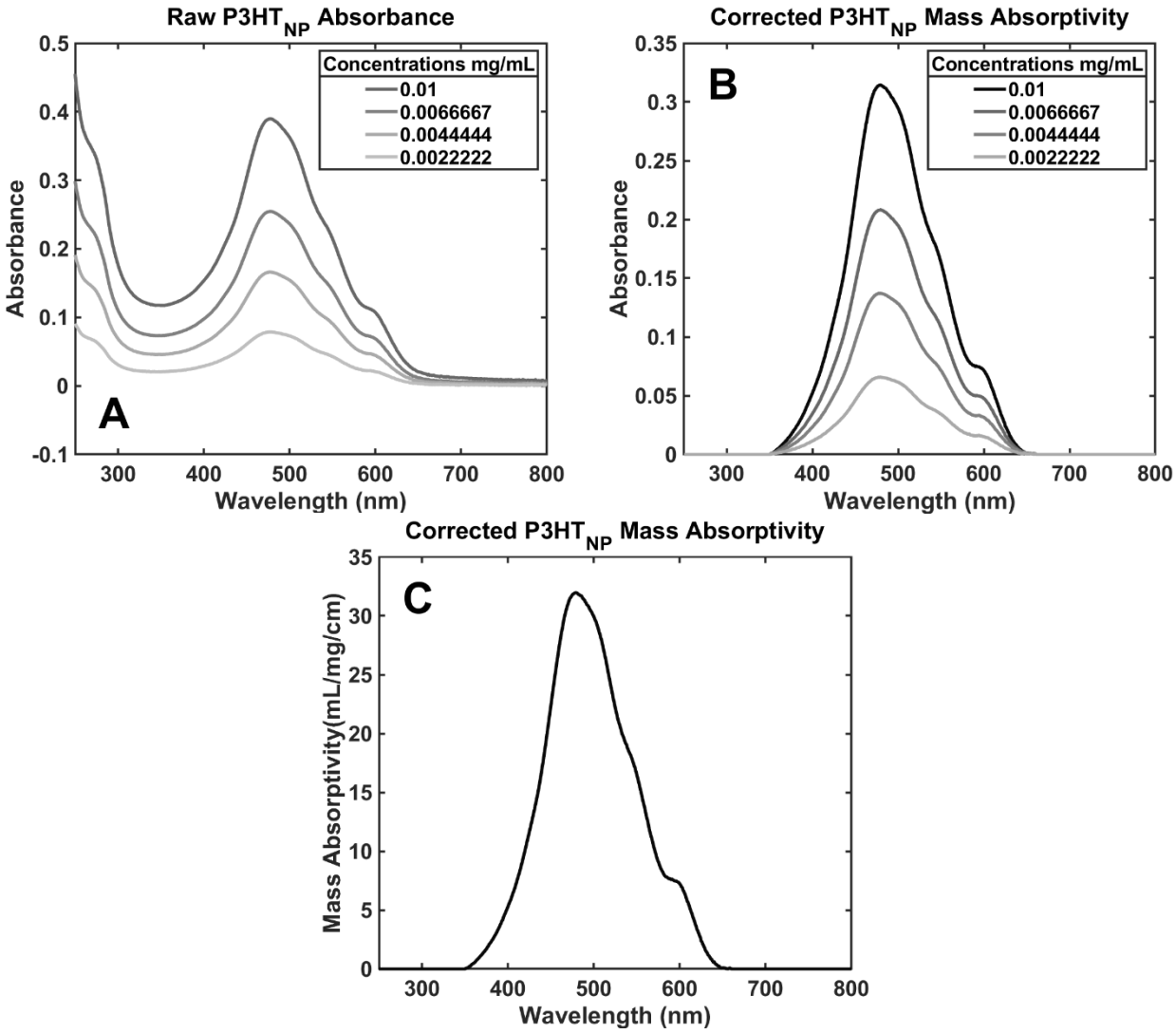

Figure S27: (a) Raw absorption data for $P3HT_{NP}$, (b) scattering background corrected absorption data for $P3HT_{NP}$, (c) mass absorptivity of $P3HT_{NP}$.

13.3 PT-Br

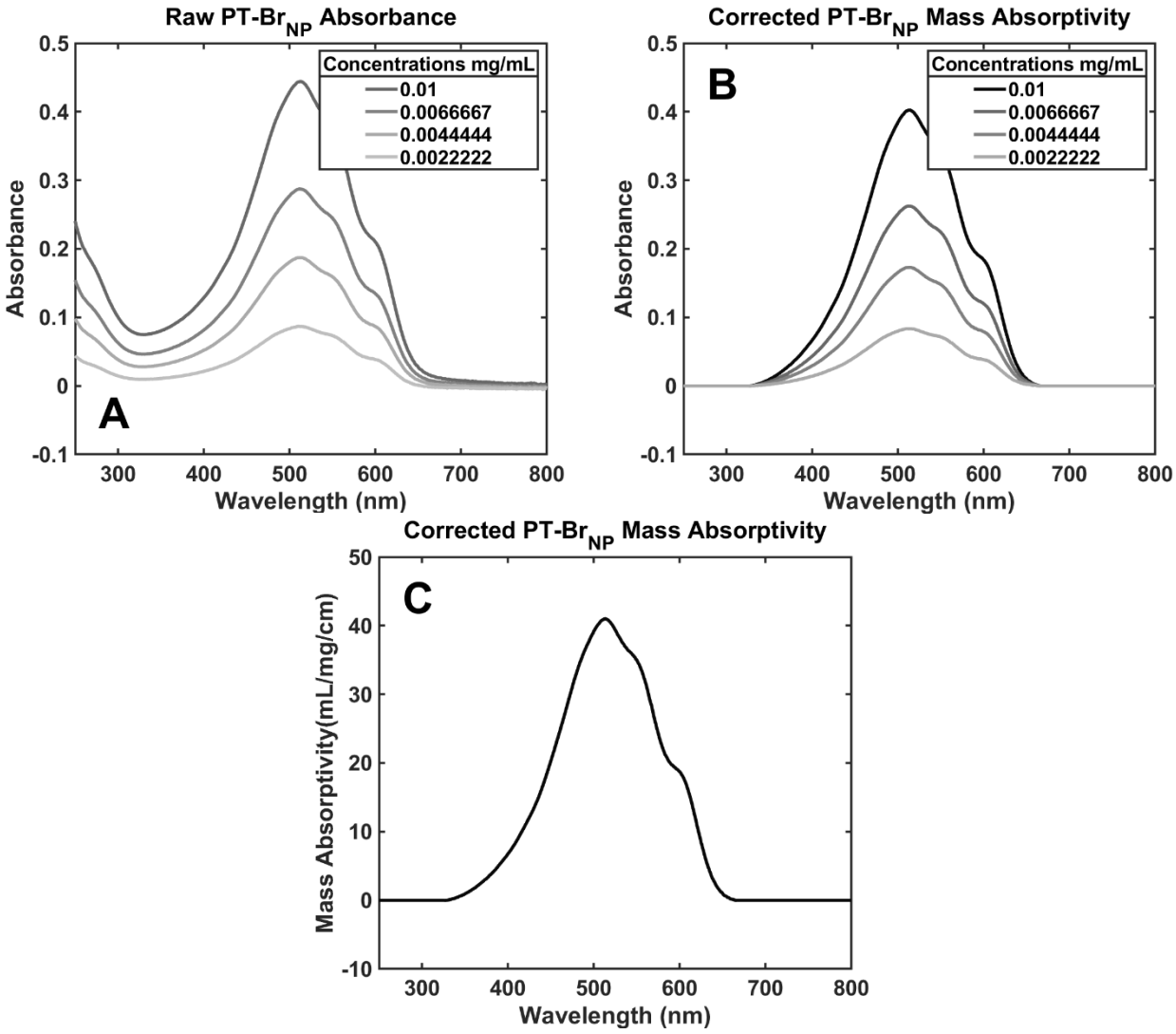

Figure S28: (a) Raw absorption data for PT-Br$_{NP}$, (b) scattering background corrected absorption data for PT-Br$_{NP}$, (c) mass absorptivity of PT-Br$_{NP}$.

13.4 PT-N_3

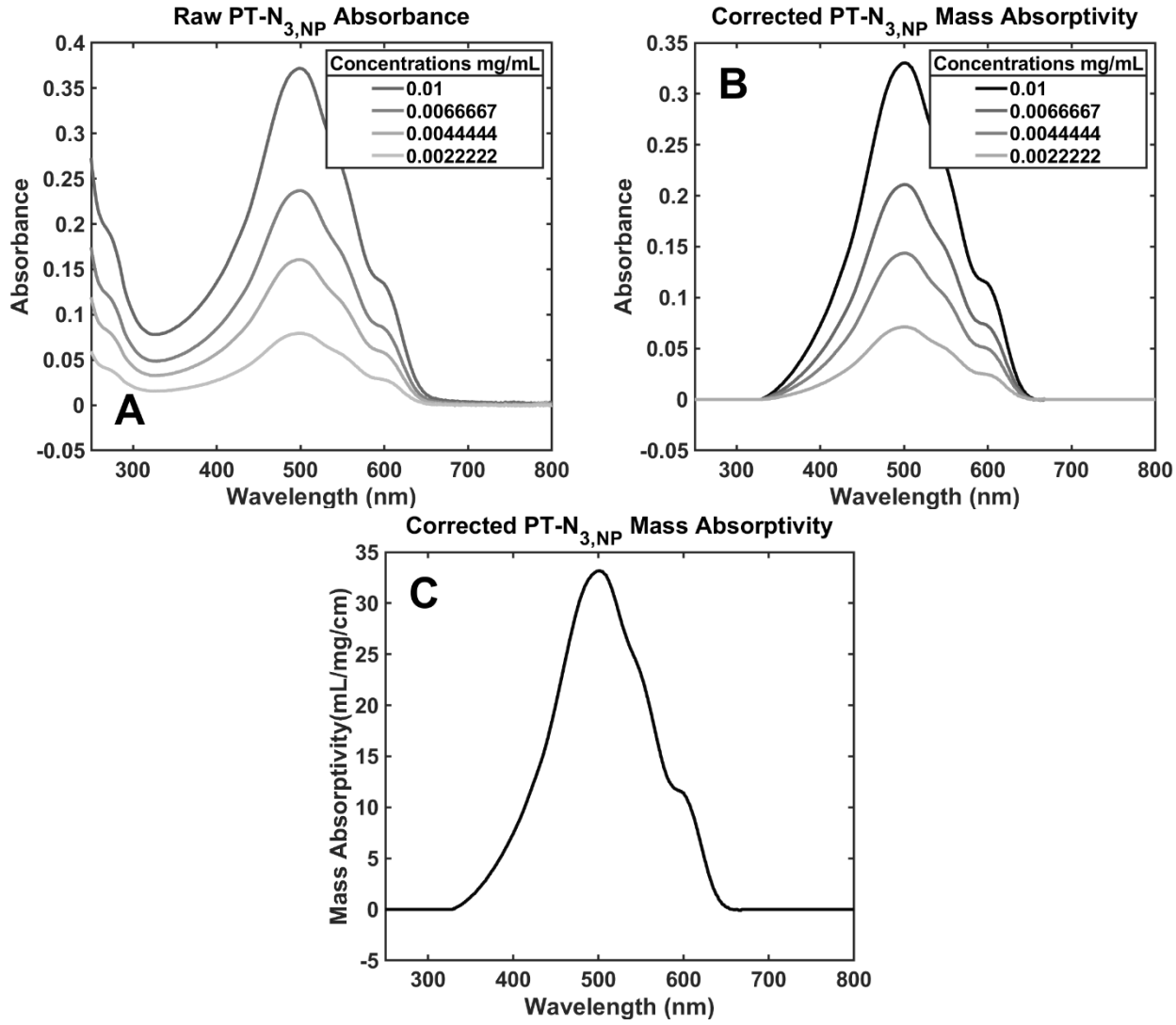

Figure S29: (a) Raw absorption data for PT-$N_{3,NP}$, (b) scattering background corrected absorption data for PT-$N_{3,NP}$, (c) mass absorptivity of PT-$N_{3,NP}$.

13.5 PT-*g*-P3HT

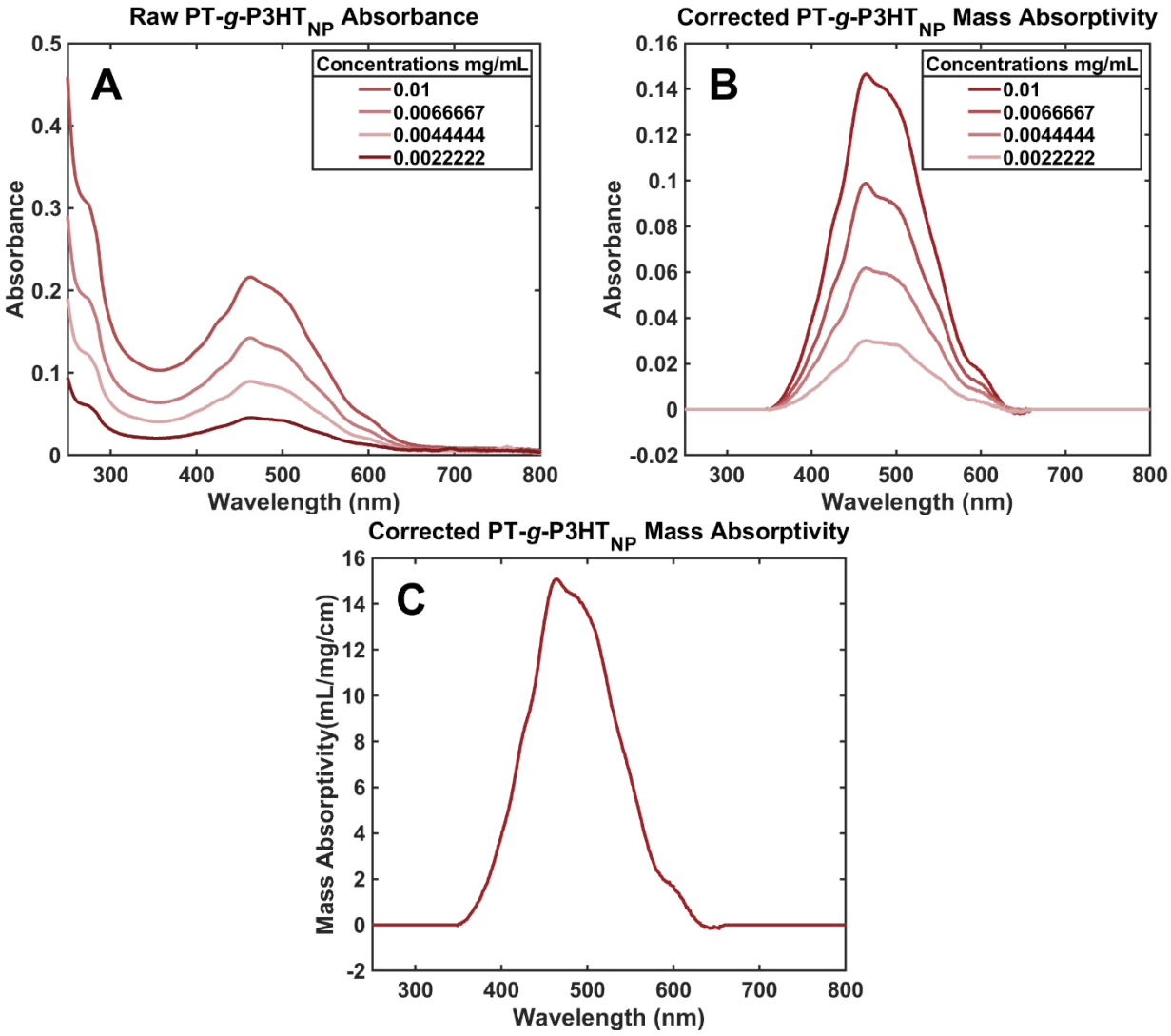

Figure S30: (a) Raw absorption data for PT-*g*-P3HT$_{NP}$, (b) scattering background corrected absorption data for PT-*g*-P3HT$_{NP}$, (c) mass absorptivity of PT-*g*-P3HT$_{NP}$.

13.6 PT-*g*-PMMA

Background subtraction from scattering effects in absorption data

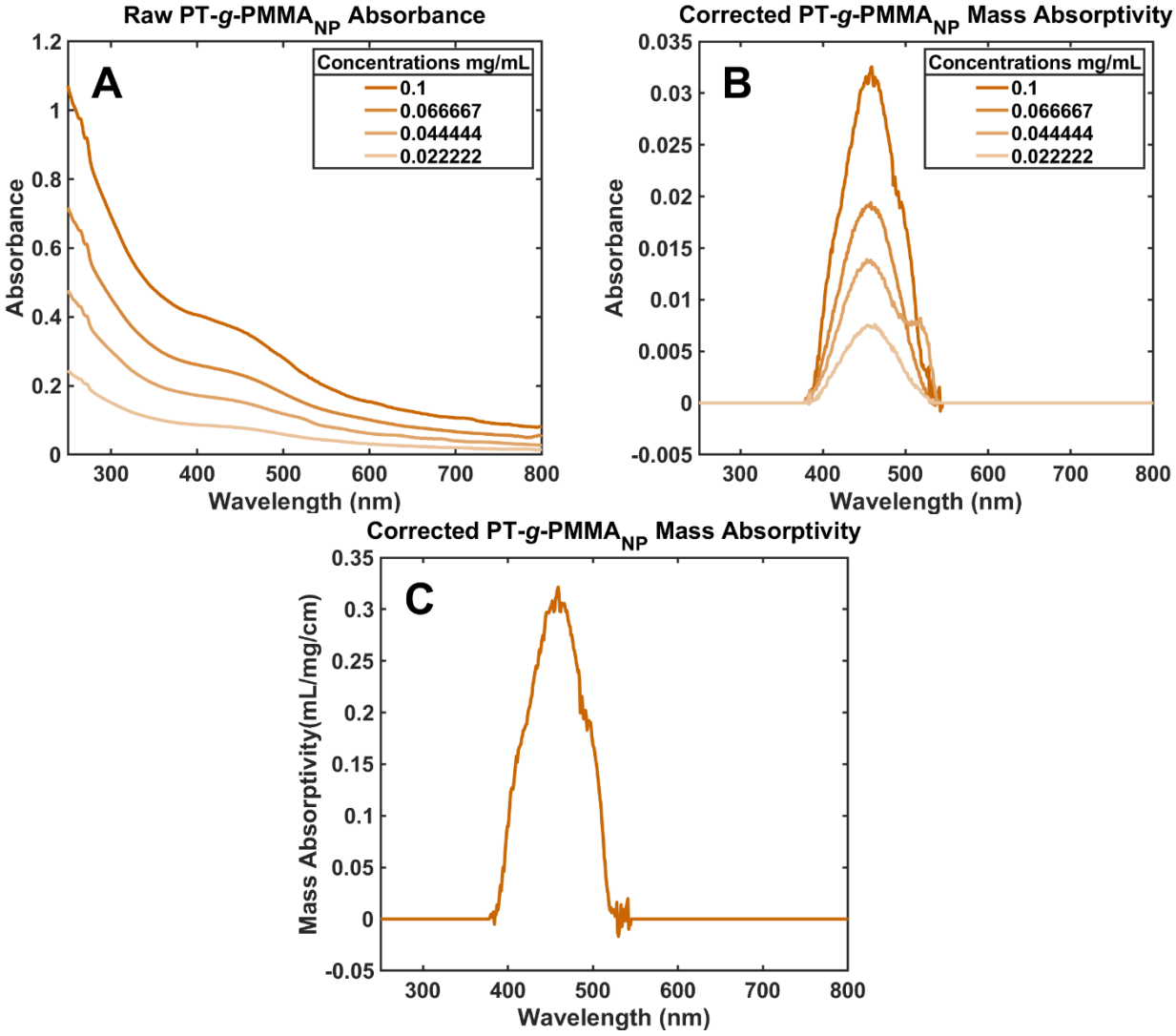

Figure S31: (a) Raw absorption data for PT-*g*-PMMA$_{NP}$, (b) scattering background corrected absorption data for PT-*g*-PMMA$_{NP}$, (c) mass absorptivity of PT-*g*-PMMA$_{NP}$.

13.7 PT-*g*-PEO

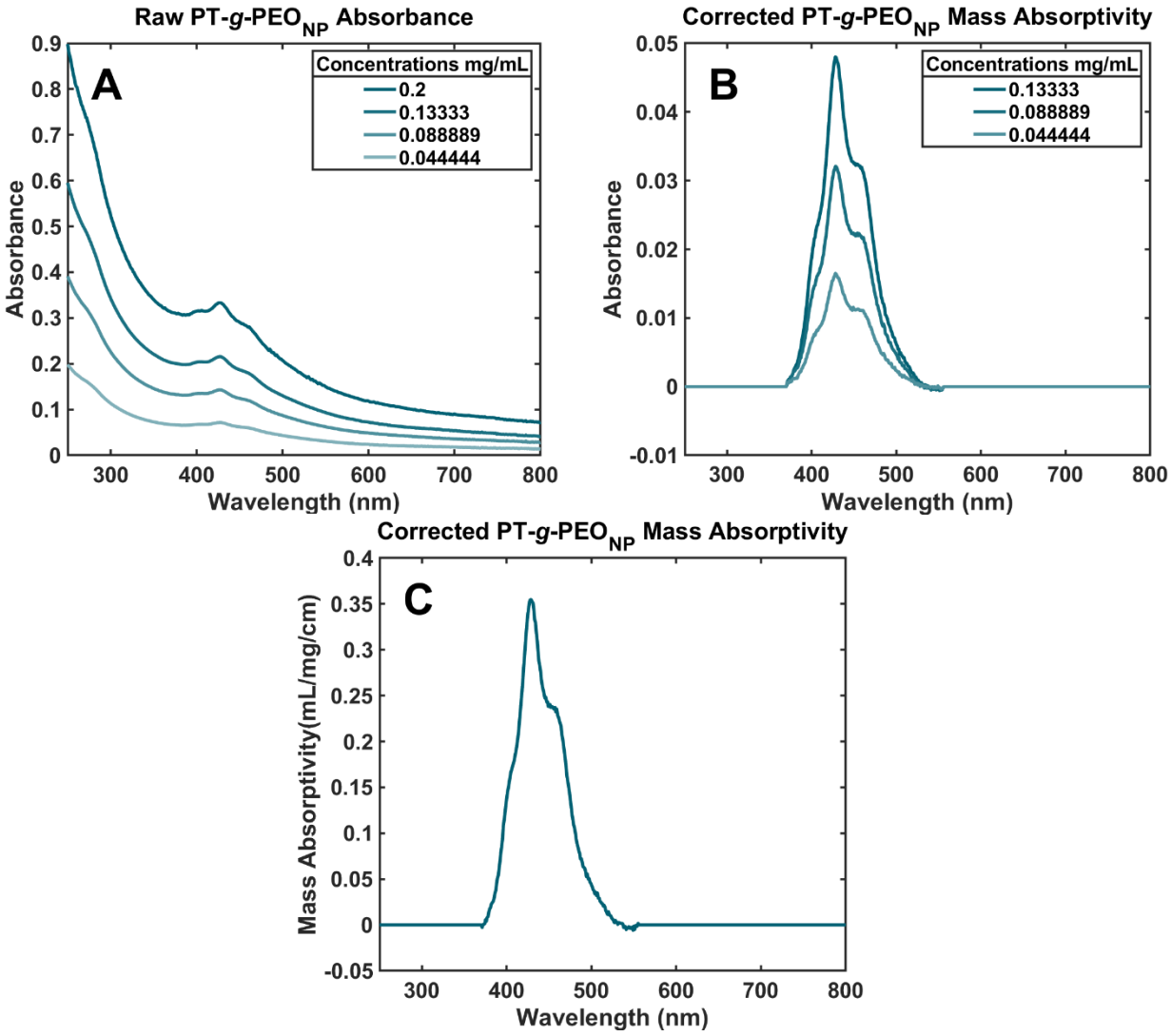

Figure S32: (a) Raw absorption data for PT-*g*-PEO$_{NP}$, (b) Scattering background corrected absorption data for PT-*g*-PEO$_{NP}$, (c) Mass absorptivity of PT-*g*-PEO$_{NP}$.

14 Quantum Yield Calculation Plots for NP solutions

14.1 P3HT

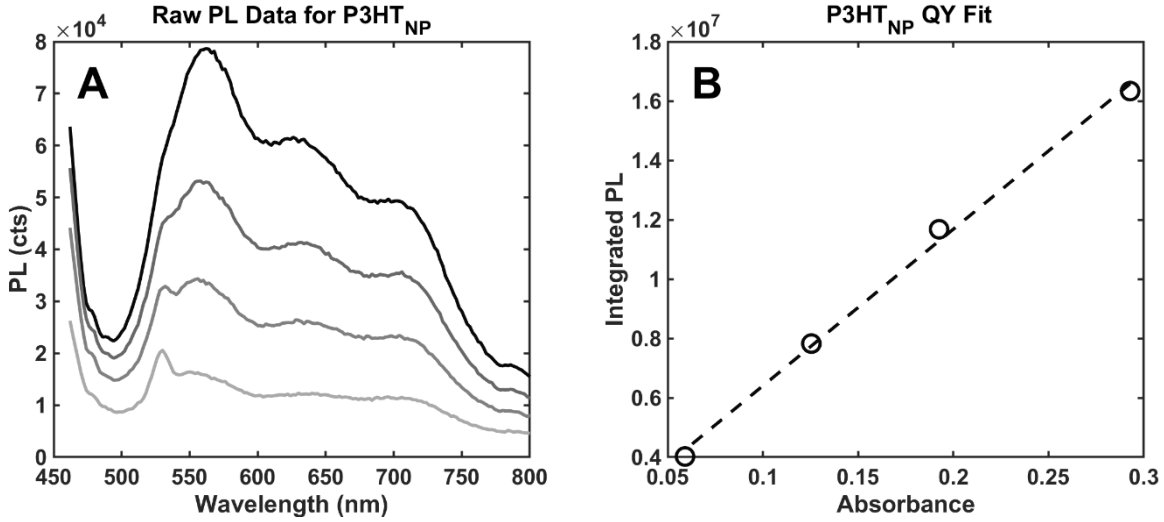

Figure S33: (a) Raw PL spectra for P3HT nanoparticles, (b) integrated fluorescence vs absorbance for P3HT nanoparticles.

14.2 PT-Br

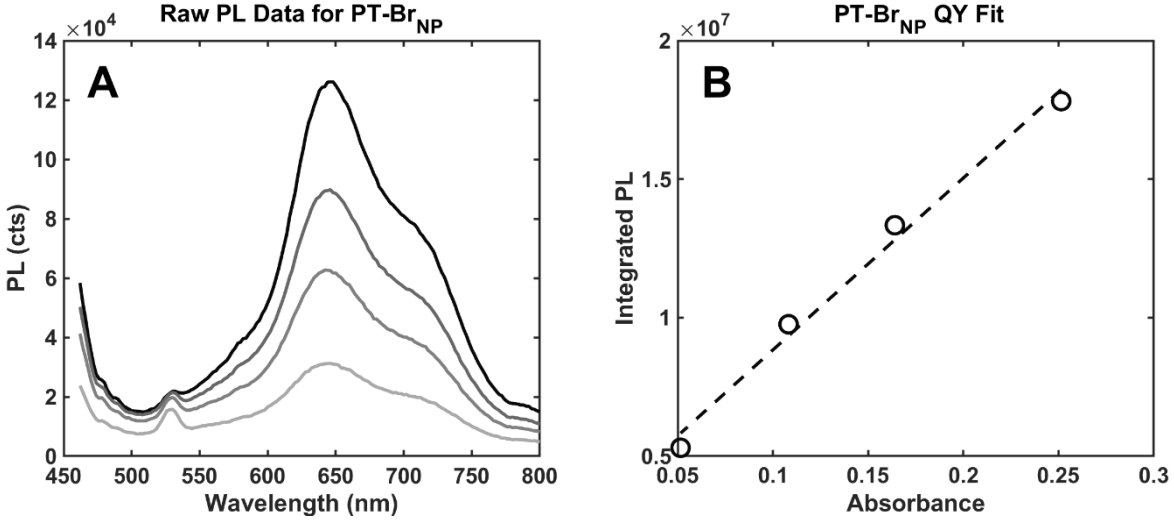

Figure S34: (a) Raw PL spectra for PT-Br nanoparticles, (b) integrated fluorescence vs absorbance for PT-Br nanoparticles.

14.3 PT-N_3

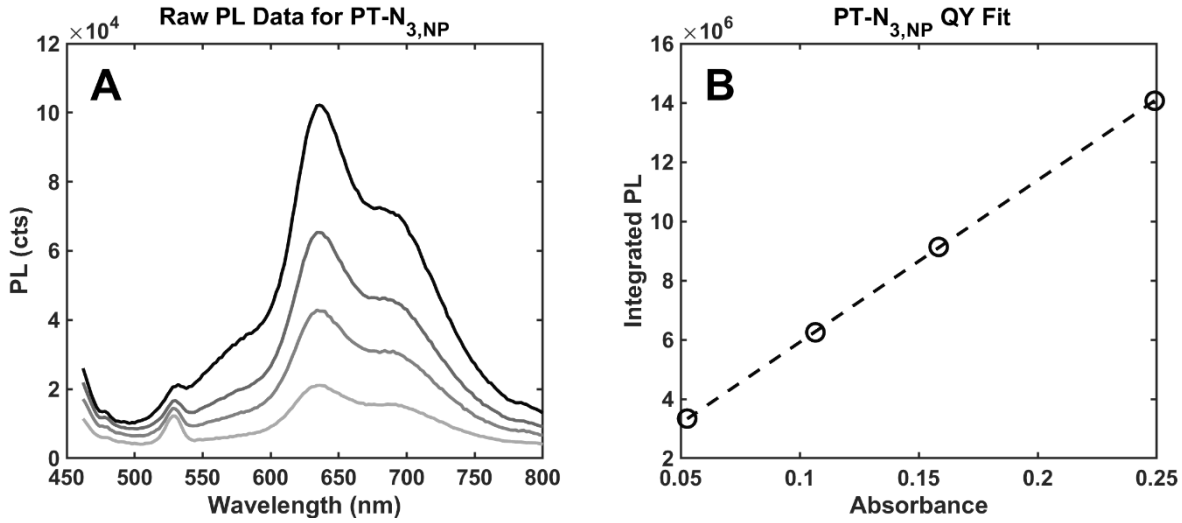

Figure S35: (a) Raw PL spectra for PT-N_3 nanoparticles, (b) integrated fluorescence vs absorbance for PT-N_3 nanoparticles.

14.4 PT-*g*-P3HT

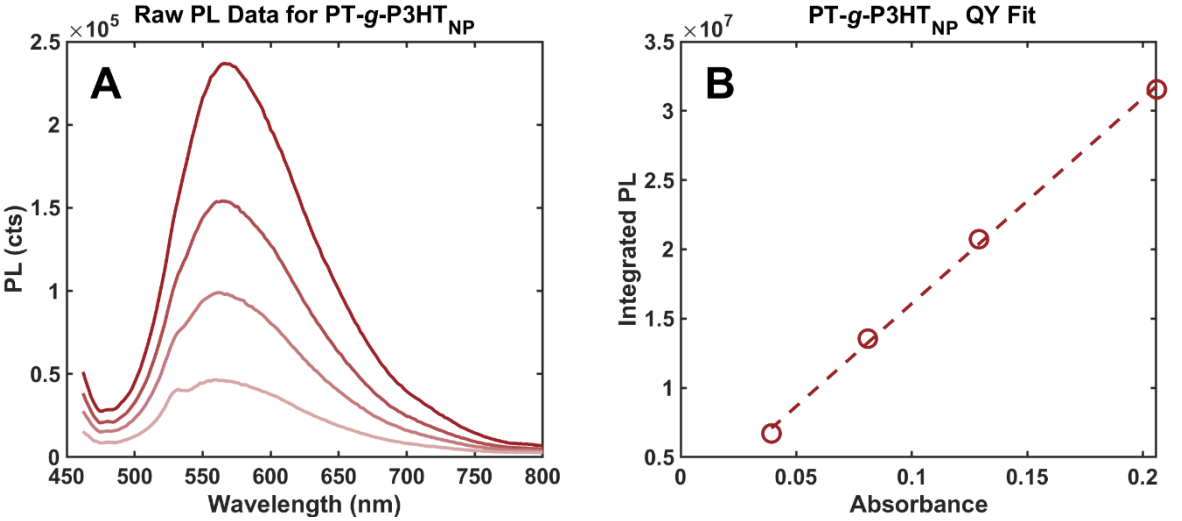

Figure S36: (a) Raw PL spectra for PT-*g*-P3HT nanoparticles, (b) integrated fluorescence vs absorbance for PT-*g*-P3HT nanoparticles.

14.5 PT-*g*-PMMA

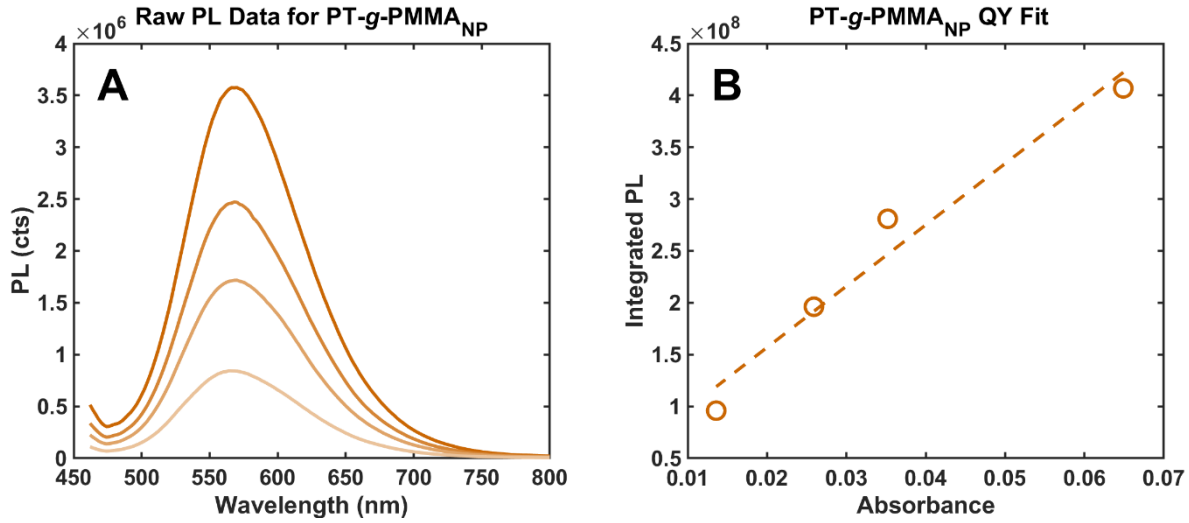

Figure S37: (a) Raw PL spectra for PT-*g*-PMMA nanoparticles, (b) integrated fluorescence vs absorbance for PT-*g*-PMMA nanoparticles.

14.6 PT-*g*-PEO

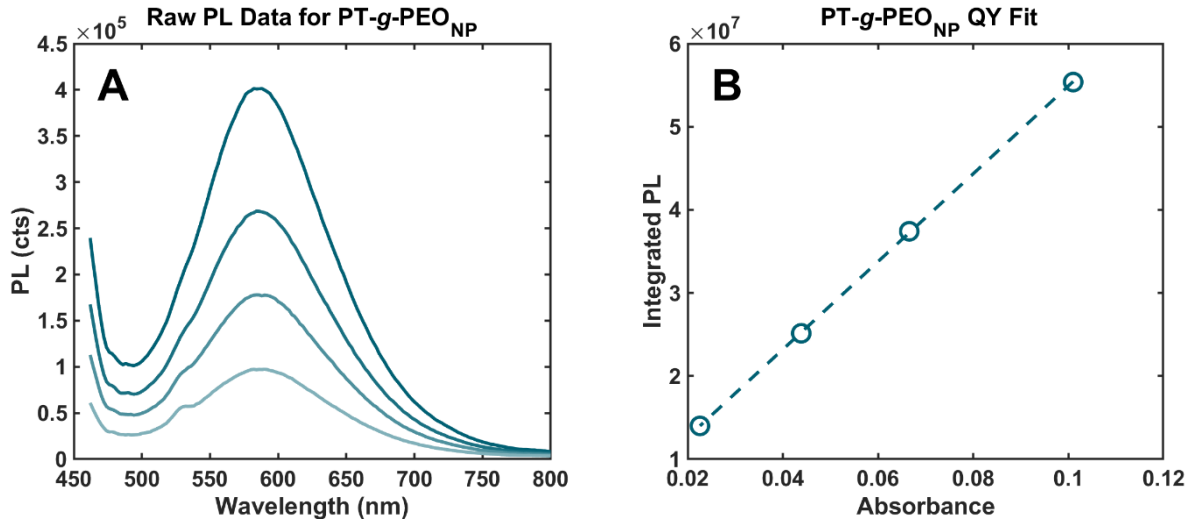

Figure S38: (a) Raw PL spectra for PT-*g*-PEO nanoparticles, (b) integrated fluorescence vs absorbance for PT-*g*-PEO nanoparticles.

15 Normalized UV-vis absorbance and fluorescence spectra for nanoparticles

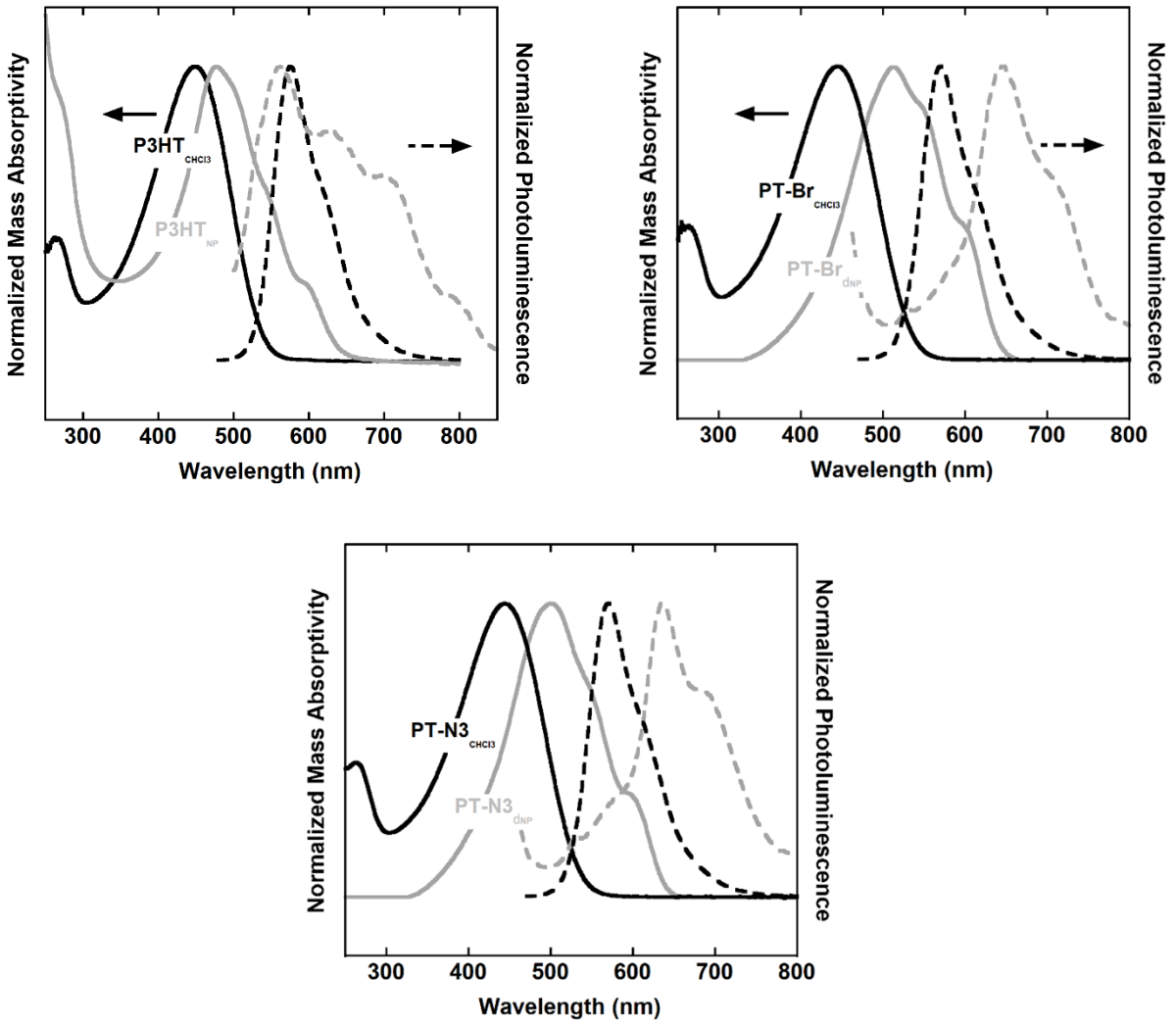

Figure S39: Normalized absorption and fluorescence in $CHCl_3$ (black) and water (grey) for (a) P3HT (b) PT-Br and, (c) PT-N_3.

16 Solid-state absorbance and photoluminescence

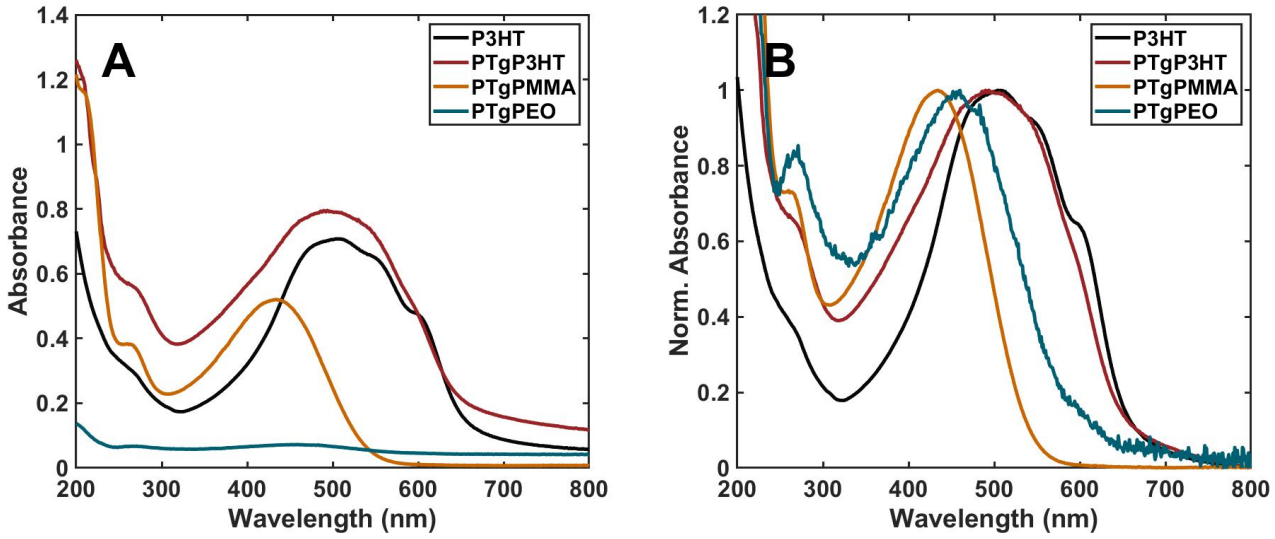

Figure S40: Solid state absorption of P3HT, PT-g-PMMA, PT-g-P3HT, PT-g-PEO (a) raw data and (b) normalized data.

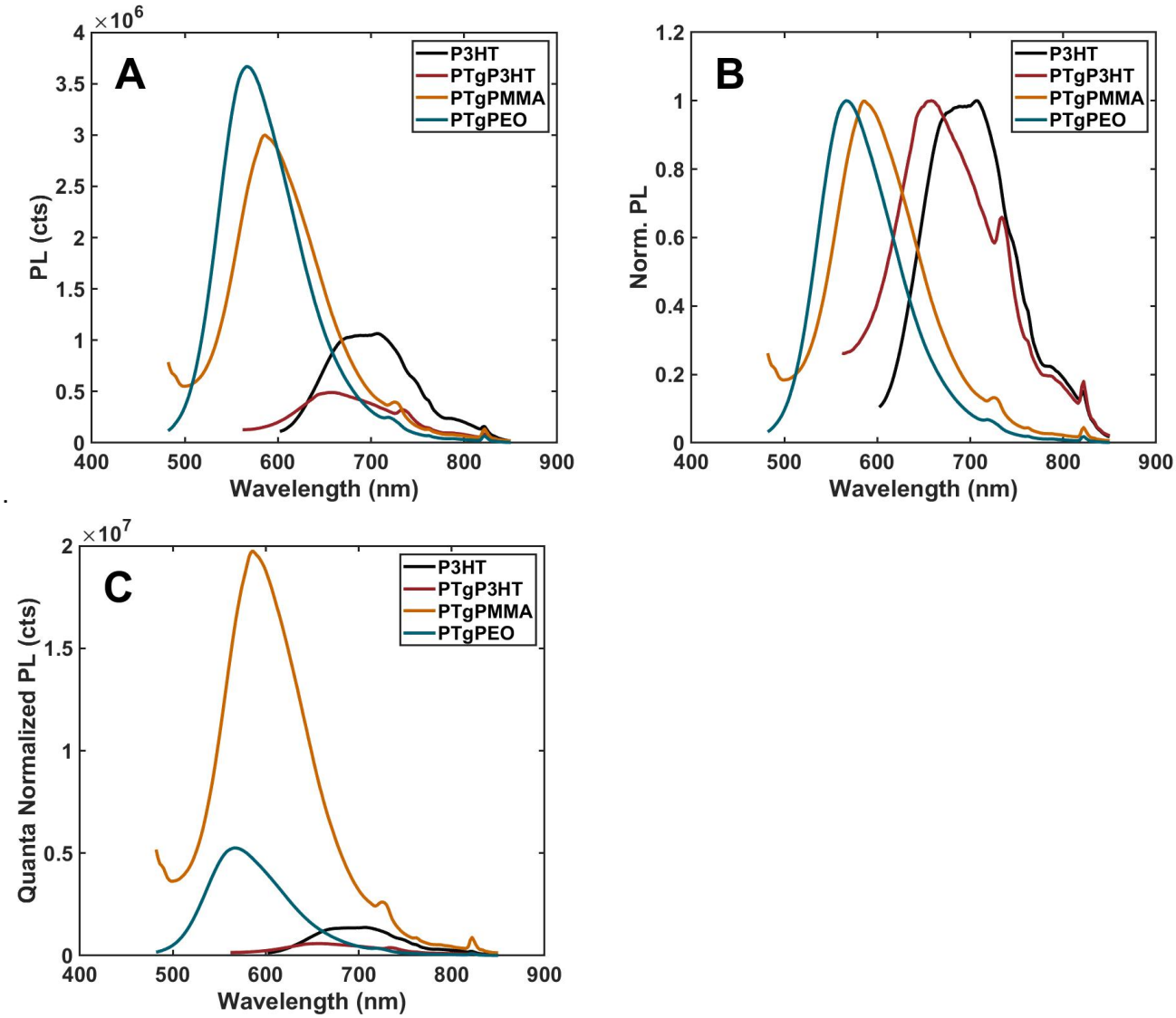

Figure S41: Photoluminescence of P3HT, PT-g-PMMA, PT-g-P3HT, PT-g-PEO (a) raw data, (b) normalized data, (c) quanta normalized data.

17 DSC of polymers

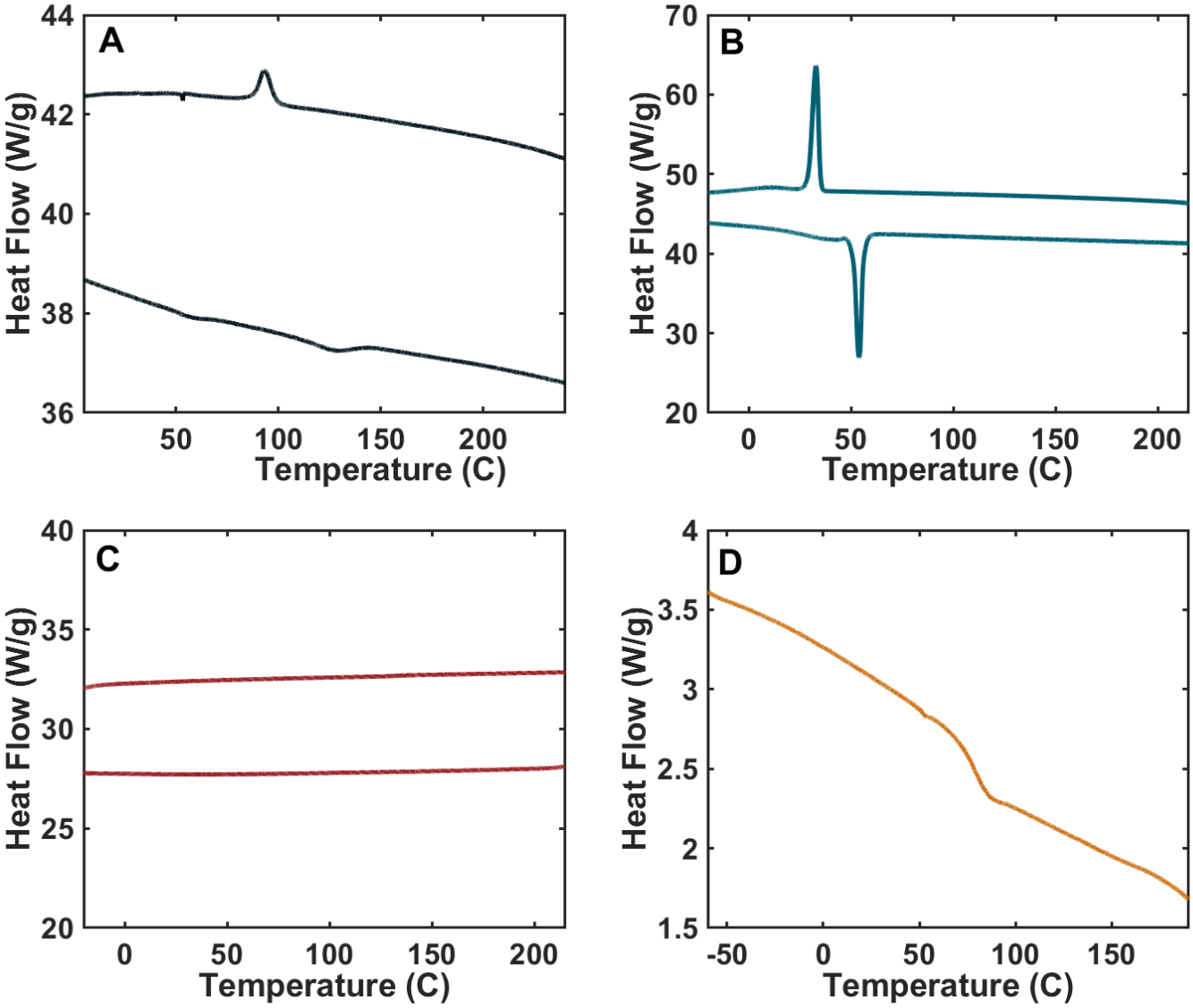

Figure S42: DSC curves for (a) P3HT, (b) PT-g-PEO, (c) PT-*g*-P3HT, and (d) PT-*g*-PMMA.

Table S6: Summarized thermal transitions of P3HT, PT-*g*-PEO, PT-*g*-P3HT, PT-*g*-PMMA.

sample	$T_g(°C)$	$T_C(°C)$	$T_m(°C)$	$\Delta Hm°$ **(J/g)**	**%crystallinity**
PEO	<-50 C*	35.7	53.8	165.2	80.6
PT-*graft*-PEO	29.0	32.9	54.0	37.37	18.2
P3HT	53.4	109.6	132.3	2.593	
PT-*graft*-P3HT	52.5	90.2	126.8	1.102	
PMMA	82.0	-	-	-	-
PT-*graft*- PMMA	78.2	-	-	-	-

18 References

[1] Y.-L. Cheng *et al.*, “Photophysical Properties of 4-(Dicyanomethylene)-2-Methyl-6-(4-Dimethylaminostyryl)-4H-Pyran (DCM) and Optical Sensing Applications,” *Intech*, p. 13, 2020, [Online]. Available: https://www.intechopen.com/books/advanced-biometric-technologies/liveness-detection-in-biometrics.

[2] S. W. Provencher, “CONTIN: A general purpose constrained regularization program for inverting noisy linear algebraic and integral equations,” *Computer Physics Communications*, vol. 27, no. 3. pp. 229–242, 1982, doi: 10.1016/0010-4655(82)90174-6.